

# Put CASH on Bandits: A Max $K$ -Armed Problem for Automated Machine Learning

Amir Rezaei Balef, Claire Vernade and Katharina Eggenberger

Department of Computer Science, University of Tübingen

{amir.rezaei-balef, claire.vernade, katharina.eggenberger}@uni-tuebingen.de

## Abstract

The Combined Algorithm Selection and Hyperparameter optimization (CASH) is a challenging resource allocation problem in the field of AutoML. We propose MaxUCB, a max  $k$ -armed bandit method to trade off exploring different model classes and conducting hyperparameter optimization. MaxUCB is specifically designed for the light-tailed and bounded reward distributions arising in this setting and, thus, provides an efficient alternative compared to classic max  $k$ -armed bandit methods assuming heavy-tailed reward distributions. We theoretically and empirically evaluate our method on four standard AutoML benchmarks, demonstrating superior performance over prior approaches.

## 1 Introduction

The performance of machine learning (ML) solutions is highly sensitive to the choice of algorithms and their hyperparameter configurations which can make finding an effective solution a challenging task. AutoML aims to reduce this complexity and make ML more accessible by automating these critical choices [Hutter et al., 2019, Baratchi et al., 2024]. For example, Hyperparameter optimization (HPO) methods focus on finding well-performing hyperparameter settings given a resource constraint, such as an iteration count or a time limit. However, in practice, it is often unclear which ML model class would perform best on a given dataset. The problem of jointly searching the model class and the appropriate hyperparameters has been coined CASH, Combined Algorithm Selection and Hyperparameter optimization [Thornton et al., 2013]. As a prime example, on tabular data, a ubiquitous data modality [van Breugel and van der Schaar, 2024], the state-of-the-art ML landscape covers classic ML methods, ensembles of gradient-boosted decision trees, and modern deep learning approaches [Kadra et al., 2021, Gorishniy et al., 2021, 2024, McElfresh et al., 2023, Kohli et al., 2024, Hollmann et al., 2023, Holzmüller et al., 2024].

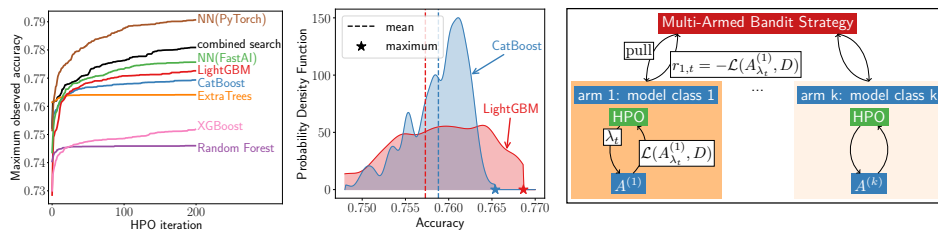


Figure 1: (Left) Running HPO for the best-performing model class (brown line) outperforms the combined search (black line), which runs HPO for the joint algorithm and hyperparameter configuration space. (Middle) The empirical performance of model classes has an irregular distribution. It is left-skewed, and a higher mean does not necessarily correspond to a higher maximum. (Right) Illustration of our approach at time step  $t$ .

A popular approach to address the CASH problem is to use categorical and conditional hyperparameters to run HPO directly on the combined hierarchical search space of models and hyperparameters. AutoML systems use this approach, which we call *combined search*, to search well-performing ML pipelines [Thornton et al., 2013, Feurer et al., 2015, Komer et al., 2014, Kotthoff et al., 2017, Feurer et al., 2022], but HPO remains inefficient in high-dimensional and hierarchical search spaces. A naive solution to address the scalability limitation is to run HPO independently for the smaller search spaces of each ML model class and then compare the found solutions. However, this solution often exceeds available computational resources and does not scale well with an increasing number of ML models. Figure 1 (left) illustrates the difference between searching each space individually (colored lines) and *combined search* (black line) on an exemplary dataset.

To leverage the efficiency of HPO in low dimensions, we use a Multi-Armed Bandit (MAB) method [Lattimore and Szepesvári, 2020] to dynamically allocate our budget. As shown in Figure 1 (left), each time the bandit strategy pulls an arm, it runs one iteration of HPO to evaluate a new configuration, resulting in a loss. The negative of the loss is used as reward feedback for the bandit algorithm. This approach is known as *decomposed CASH* [Hoffman et al., 2014, Liu et al., 2019].

While most classical MAB problems aim to maximize the average rewards over time, the goal of the bandit algorithm for *decomposed CASH* should be to maximize the maximum reward observed over time: as illustrated in Figure 1 (middle), tuning the LightGBM (red) will eventually outperform CatBoost. This goal aligns with Max  $K$ -Armed Bandit (MKB) problems [Carpentier and Valko, 2014, Achab et al., 2017, Baudry et al., 2022], often referred to as Extreme Bandits.

In the context of AutoML, the time horizon is limited, making efficiency crucial. Prior work on *decomposed CASH* found that state-of-the-art MKB algorithms are not sufficiently sample-efficient in practice [Hu et al., 2021, Balef et al., 2024]. Additionally, Nishihara et al. [2016] argued that the parametric assumptions derived from extreme value theory are not applicable in the context of HPO and stated that “the question of what realistic assumptions are likely to hold in practice for hyperparameter optimization is an important question”.

We precisely address this open question through a thorough statistical analysis of the empirical reward distributions of HPO tasks. Our data-driven approach reveals that common assumptions used in MKB problems do *not* hold in this context, and we define new ones for MaxUCB, an MKB algorithm for bounded light-tailed reward distributions. Concretely, our contributions are as follows:

1. We study the empirical reward distributions in HPO tasks and observe that they follow negatively skewed bounded distributions (left-skewed or left-tailed reward distributions).
2. We propose an appropriate MKB algorithm, MaxUCB, for this newly defined setting.
3. We provide a regret bound and theoretical analysis for MaxUCB, showing that the number of sub-optimal trials grows sub-linearly with time.
4. Finally, we demonstrate superior empirical performance on four popular AutoML benchmark tasks where we compare MaxUCB with state-of-the-art MAB algorithms developed for AutoML, and *combined search*.

Our main contribution is a state-of-the-art algorithm for decomposed CASH based on a novel extreme bandit algorithm we call MaxUCB (Algorithm 1). We demonstrate the performance of our method on four benchmarks, which highlight the relevance of our assumptions for a wide variety of CASH problems. We analyze the theoretical performance of MaxUCB (Theorem 4.2) through high-probability regret bounds that also justify our novel choice of exploration bonus for the type of distributions resulting from the CASH problem. Importantly, our objective is rather to propose a practical algorithm with good empirical performance on CASH rather than a general multi-purpose bandit algorithm, so our guarantees hold under carefully crafted assumptions that resolve previously open questions [Nishihara et al., 2016].

## 2 Solving CASH using Bandits

The CASH problem for supervised learning tasks is defined as follows [Thornton et al., 2013]. Given a dataset  $\mathbb{D} = \{D_{train}, D_{valid}\}$  of a supervised learning task, let  $\mathcal{A} = \{A^{(1)}, \dots, A^{(K)}\}$  be the set of  $K$  candidate ML algorithms, where each algorithm  $A^{(i)}$  has its own hyperparameter search space  $\Lambda^{(i)}$ . The goal is to search the joint algorithm and hyperparameter configuration space to find the optimal algorithm  $A^{(i^*)}$  and its optimal hyperparameter configuration  $\lambda^*$  that minimizes a loss metric

$\mathcal{L}$ , e.g., the validation error<sup>1</sup>. Formally,

$$A_{\lambda^*}^{(i^*)} \in \arg \min_{A^{(i)} \in \mathcal{A}, \lambda \in \Lambda^{(i)}} \mathcal{L}(A_{\lambda}^{(i)}, \mathbb{D}). \quad (1)$$

For our approach, we study the decomposed variant [Hoffman et al., 2014, Liu et al., 2019], which yields the following bilevel optimization problem depicted in Figure 1 (right): at the upper level, we aim to find the overall best-performing ML model  $A^{(i^*)}$  by selecting model  $A^{(i)} \in \mathcal{A}$  iteratively, and at the lower level, we aim to find the best-performing configuration  $\lambda^* \in \Lambda^{(i)}$  for the selected model  $A^{(i)}$ . Formally,

$$A^{(i^*)} \in \arg \min_{A^{(i)} \in \mathcal{A}} \mathcal{L}(A_{\lambda^*}^{(i)}, \mathbb{D}), \quad \text{s.t.} \quad \lambda^* \in \arg \min_{\lambda \in \Lambda^{(i)}} \mathcal{L}(A_{\lambda}^{(i)}, \mathbb{D}) \quad (2)$$

The right-hand side of Equation 2 in the lower level can be efficiently addressed by existing iterative HPO methods such as Bayesian optimization (BO) [Jones et al., 1998, Garnett, 2022], which has been demonstrated to perform well in practical settings [Snoek et al., 2012, Chen et al., 2018, Cowen-Rivers et al., 2022]. BO fits a surrogate model and uses an acquisition function to find a promising configuration to evaluate next. The left-hand side of Equation 2, corresponding to the upper level, has to trade off exploration and exploitation of HPO runs, a typical MAB problem as already noticed in prior work [Cicirello and Smith, 2005, Streeter and Smith, 2006a, Nishihara et al., 2016, Metelli et al., 2022].

We denote  $\lambda_t$  the configuration proposed by the HPO method in the lower level and  $r_{i,t}$  to be the feedback to arm  $i$  obtained by evaluating  $\lambda_t \in \Lambda^{(i)}$  at time step  $t \leq T$ . To be consistent with the bandit literature, we consider the negative loss as the reward and maximize it:

$$r_{i,t} = -\mathcal{L}(A_{\lambda_t}^{(i)}, \mathbb{D}). \quad (3)$$

The goal is then to find the best-performing algorithm  $A^{(i^*)}$  and its optimal configuration  $\lambda^*$  under a budget constraint  $T$ . This can be framed as minimizing the regret  $R(T)$  with  $I_t$  being the selected arm at time  $t$  by:

$$R(T) = \max_{k \leq K} \mathbb{E}[\max_{t \leq T} r_{k,t}] - \mathbb{E}[\max_{t \leq T} r_{I_t,t}]. \quad (4)$$

This regret describes the gap between the highest-possible oracle reward that could be obtained by pulling only the arm with the highest performance (left part) and the actual observed rewards obtained by applying our strategy (right part). Notably, the expectation is necessary to account for the inherent stochasticity of both the HPO procedure (e.g., random search or Bayesian optimization) and the ML models themselves (e.g., random initialization and training variability).

Instead of using MKB algorithms to directly address Equation 4, closely related prior works focus on alternative methods. For example, Hu et al. [2021] proposed and analyzed the *Extreme-Region Upper Confidence Bounds (ER-UCB)* algorithm maximizing the extreme-region of the feedback distribution, assuming Gaussian rewards.

More recently, Balef et al. [2024] have shown that existing MKB algorithms underperform when applied to *decomposed CASH*, and they proposed methods for maximizing the quantile values instead of the maximum value.

As another alternative method, Li et al. [2020] framed the CASH problem as a Best Arm Identification (BAI) task and introduced the *Rising Bandits* algorithm [Li et al., 2020].

This MAB method assumes that the reward function for each arm increases with each pull, following a rested bandit model with non-decreasing payoffs [Heidari et al., 2016] (which has been shown to have linear regret when the reward increment per pull exceeds a threshold [Metelli et al., 2022]). *Rising Bandits* can be used for our setting using the maximum observed performance of the HPO history as the reward. However, this algorithm assumes deterministic rewards and increasing concave reward functions. To weaken this assumption, Li et al. [2020] introduced a hyperparameter to increase

<sup>1</sup>We note that  $\mathcal{L}$  can also be the result of k-fold cross-validation or other evaluation protocols measuring the expected performance of a model on unseen data [Raschka, 2018].

initial exploration. [Mussi et al. \[2024\]](#) further weakened this assumption by assuming that the moving average of the rewards is an increasing concave function.

Generally, in BAI approaches, the main goal is to identify the arm with the highest mean reward. The learner can freely use its resources to explore the arms and get a noisy observation of their mean value, but must eventually stop and output a single arm. This objective differs from ours and is ill-suited for CASH because the best algorithm has the best achievable performance rather than the best performance on average over hyperparameters.

### 3 Data Analysis of HPO Tasks

Here, we analyze and empirically examine our problem’s reward distributions. In our setup, the reward corresponds to the performance of the hyperparameter configurations obtained by running HPO. To illustrate the reward distributions, for each ML model class (corresponding to arms in our setup), we run  $T = 200$  iterations of HPO, with 32 repetitions (each using a different seed) on a varying number of datasets on four AutoML benchmarks (see Appendix [D.2](#) and [C.1](#)).

We begin by analyzing our reward characteristics through the *survival function*  $G$  of the distribution  $d$  defined as:

$$\forall x \in \mathbb{R}, \quad G(x) = P_{X \sim d}(X \geq x).$$

Figure 2 shows the average empirical survival function of all observed performances (normalized between 0 and 1 for each task) for each arm. We rank model classes (i.e., arms) based on their best performance per dataset and report results on two benchmarks. We observe that the reward distributions are

1. **bounded.** The reward, which measures the performance of a model, is determined by a score metric, e.g., accuracy. The extreme values vary for each arm and depend on the capability of the model class and the complexity of the task. Therefore, even if we run HPO indefinitely, achieving an infinite reward is impossible. Consequently, each arm has a bounded support with different maximum values, and at least a single optimal arm exists. → **We can define a sub-optimality gap (Definition 3.1).**
2. **short-tailed, left-skewed, and the right tail is not heavy.** The rewards are concentrated near the maximal value per model class, and extreme events are not outliers. As the HPO method’s performance reaches a certain level, further optimization often yields only small gains as optima tend to have flat regions [[Pushak and Hoos, 2022](#)]. Therefore, many configurations perform similarly well, resulting in a skewed distribution.<sup>2</sup> → **We expect to observe many extreme rewards.**
3. **nearly stationary.** This means that the optimal arm does not change over time. This is clear for TabRepoRaw. We observe significant changes in the distributions for YaHPOGym, but most of the sub-optimal arms remain sub-optimal over time. → **Ranking of well-performing arms does not change over time.**

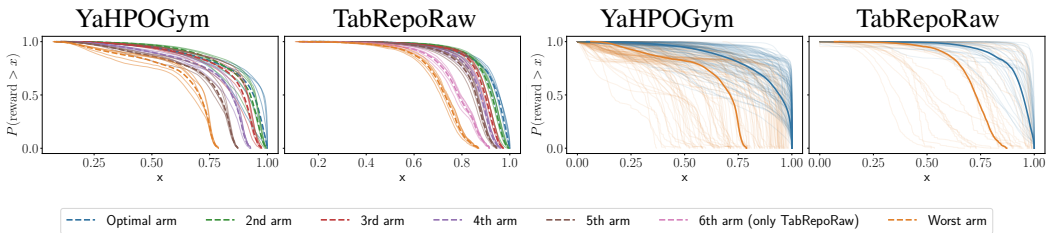


Figure 2: (Left two plots) The average empirical survival function of the reward distribution per arm ranked per dataset. Thin lines correspond to segments of the reward sequence and show the distribution change over time. (Right two plots) The average empirical survival function per dataset for the best and worst arm. Thin lines correspond to individual datasets.

<sup>2</sup>This has also been observed for related tasks, e.g., neural architecture search on CIFAR-10 [[Su et al., 2021](#)].

Prior research has shown that existing MKB algorithms can underperform if their assumptions about the distributions are too weak or misaligned [Nishihara et al., 2016, Balef et al., 2024]. This underperformance is largely due to our second observation, which significantly differs from the common assumptions of the existing algorithms.

**Preliminaries.** Based on these observations, we can formulate the following definition and assumption on which we develop and analyze our algorithm.

**Definition 3.1.** The *suboptimality gap*  $\Delta_i \geq 0$  for arm  $i$  is defined as:

$$\Delta_i = \mathbb{E} \left[ \max_{t \leq T} r_{i^*,t} \right] - \mathbb{E} \left[ \max_{t \leq T} r_{i,t} \right]$$

where  $r_{i^*,t}$  and  $r_{i,t}$  are the rewards observed from optimal arm  $i^*$  and arm  $i$  at time  $t$ , respectively.

**Assumption 3.2.** We assume that the i.i.d. random variable  $X$ , representing the rewards, follows a bounded distribution with support in  $[a, b]$  and continuous survival function  $G$ .

**Lemma 3.3.** Suppose Assumption 3.2 holds. Then, there exists  $L, U \geq 0$  such that the survival function  $G$  can be bounded near  $b$  by two linear functions.

$$\forall \epsilon \in (0, b - a), \quad L\epsilon \leq G(b - \epsilon) \leq U\epsilon \quad (5)$$

Lemma 3.3 (proof in Appendix B.1) provides a way to characterize the shape of any bounded distribution near its maximum value through distribution-dependent constants,  $L$  and  $U$

(see Appendix C.2 for more details and a visualization). Intuitively, it quantifies the behavior of the distribution of the ML model performance in a given hyperparameter space near the optimum. A large value of  $L$  indicates a steep drop in the survival function near the maximum, while a small value of  $U$  leads to a more gradual decay of the survival function and conversely (see Figure 3).

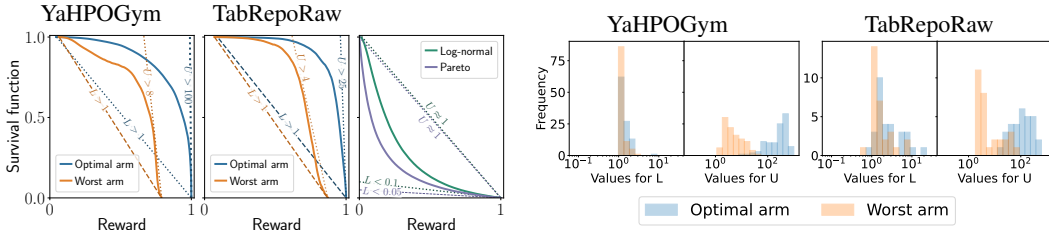


Figure 3: (Left, Middle)  $L$  and  $U$  for the average survival functions in Figure 2. (Right) We highlight the difference to right-skewed Log-normal and Pareto distributions.

Figure 4:  $L$  and  $U$  values across individual datasets.

We study the values of  $L$  and  $U$  in Lemma 3.3 on our empirical data and show the distribution of  $L$  and  $U$  in Figure 4 (see Appendix C.3 for more analyses). Next, we focus on the uniqueness of our assumptions before discussing how this impacts our MKB algorithm’s performance in Section 4.

**Common Max  $K$ -armed Bandit assumptions are misaligned with CASH.** Existing MKB algorithms can be classified into two main categories. First, distribution-free approaches do not leverage any assumption on the type of reward distributions [Streeter and Smith, 2006b, Bhatt et al., 2022, Baudry et al., 2022]. Secondly, parametric and semi-parametric approaches typically assume that the reward distributions follow heavy-tailed distributions, typically following a second-order Pareto assumption whose parameters can be estimated using extreme value theory [Carpentier and Valko, 2014, Achab et al., 2017].

Our empirical analysis shows that existing MKB algorithms’ assumptions about reward distributions are either overly broad or misaligned with the CASH problem. We identify two key differences between our assumptions and those made by current MKB algorithms. First, the sub-optimality gap makes the regret definition (Equation 4) for bounded distributions meaningful. Without the existence of a nonzero gap, the regret definition fails since any policy consistently selecting a single arm can achieve zero regret, as Nishihara et al. [2016] pointed out with Bernoulli distributions. Second, our reward distributions differ from those used in existing MKB algorithms. Lemma 3.3

characterizes the shape of the distribution, with a higher  $L$  ensuring more mass near extreme values, making extreme values easier to estimate. In our case, values for  $L$  are mostly higher than 1 while for heavy-tailed distributions, commonly used as the basis in existing MKB algorithms, are close to 0 (see the rightmost plot in Figure 3). In general, our analysis shows that considering the right range of  $L$  values unlocks the problem raised by Nishihara et al. [2016], who focused on constructing counterexamples through the distributions that have absurd values for  $L$ . Thus, Theorem 11, “no policy can be guaranteed to perform asymptotically as well as an oracle that plays the single best arm for a given time horizon.”, which means any policy needs to explore all arms for budget  $T$ , does not apply here.

## 4 MaxUCB

Based on Lemma 3.3 and the regret definition (Equation 4), we introduce MaxUCB in Algorithm 1 for  $K$  arms with a limited time horizon of  $T$  iterations.<sup>3</sup>

**Description of MaxUCB.** Our algorithm balances exploration and exploitation according to the standard optimism principle at the heart of Upper Confidence Bound (UCB) bandit methods [Auer, 2002, Lattimore and Szepesvári, 2020]. The main novelty we introduce is in the computation of a distribution-adapted exploration bonus for MaxUCB.

Our exploration bonus  $(\frac{\alpha \log(t)}{n})^2$  deviates from typical UCB literature due to faster concentration of maximum values in bounded distributions. The probability of bad events (see Equation 31 in Appendix B.3) can be written as:

$$P(\text{Bad events}) \leq e^{-n\sqrt{C(n)}} + nC(n). \quad (6)$$

Then, setting  $C(n) = 1/n^2$  minimizes the probability of bad events: the first term becomes independent of  $n$ , while the second term decreases with  $n$ . Furthermore, MaxUCB uses  $\alpha \geq 0$  to control the exploration-exploitation trade-off; a higher  $\alpha$  leads to more exploration.

---

### Algorithm 1 MaxUCB

---

**Require:**  $\alpha$ (exploration parameter),  $T$ (time horizon),  $K$ (arms)

- 1: **for** each arm  $i \leq K$  **do**
- 2:   Pull arm  $i$ , set  $n_i \leftarrow 1$ , observe reward  $r_{i,1}$  ▷ Evaluating default configuration
- 3: **end for**
- 4: **for**  $t = K + 1$  to  $T$  **do**
- 5:   **for** each arm  $i \leq K$  **do**
- 6:     Update policy  $U_i = \max(r_{i,1}, \dots, r_{i,n_i}) + (\frac{\alpha \log(t)}{n_i})^2$
- 7:   **end for**
- 8:   Select arm  $I_t = \arg \max_{i \leq K} U_i$ ,  $n_{I_t} \leftarrow n_{I_t} + 1$ , then observe reward  $r_{I_t, n_{I_t}}$
- 9: **end for**

---

### Analysis of MaxUCB.

We first show a regret decomposition result specific to max- $K$  armed bandits (Proposition 4.1) that directly relates the regret definition in equation 4 with the number of suboptimal trials.

**Proposition 4.1.** (Upper Regret Bound) *the upper regret bound up to time  $T$  is related to the number of times sub-optimal arms are pulled,*

$$R(T) \leq \frac{\max_{i \leq K} b_i}{T} \sum_{i \neq i^*}^K N_i(T) \quad (7)$$

Where  $N_i(T) = \mathbb{E}(\sum_{t=1}^T \mathbb{1}\{I_t = i\})$  is the number of sub-optimal pulls of arm  $i$ , arm  $i^*$  is the optimal arm and  $b_i$  is the upper bound on the reward of arm  $i$  as given by Assumption 3.2, i.e., the reward of arm  $i$  lies within the interval  $[a_i, b_i]$ .

---

<sup>3</sup>MaxUCB needs to store the number of pulls and the maximum reward for each arm, resulting in a memory requirement of  $\mathcal{O}(K)$ . The time complexity is  $\mathcal{O}(KT)$ .

The proof is provided in Appendix B.2 and relies on standard tools in the extreme bandit literature [Baudry et al., 2022]. From this result, it is clear that we can now obtain an upper bound on the regret by controlling the number of suboptimal arm pulls  $(N_i(T))_{i \neq i^*}$  individually. Our main theoretical result below proves such an upper bound for Algorithm 1.

**Theorem 4.2.** *For any suboptimal arm  $i \neq i^*$ , the number of suboptimal draws  $N_i(T)$  performed by MaxUCB (Algorithm 1) up to time  $T$  is bounded by*

$$N_i(T) \leq \frac{T^{1-2L_{i^*} \alpha \sqrt{\Delta_i}}}{1 - 2L_{i^*} \alpha \sqrt{\Delta_i}} + 2\alpha \sqrt{U_i T} \log(T) \quad (8)$$

The result of Theorem 4.2 (proof provided in Appendix B.3) highlights that MaxUCB primarily leverages two key properties: the sub-optimality gap  $\Delta_i$  and the shape of the distribution, as defined in Lemma 3.3. Specifically, the performance improves with a larger value for  $\Delta_i$  (the sub-optimality gap) and higher values of  $L_{i^*}$  ( $L$  for the optimal arm), which means that samples drawn from the distribution of the optimal arm are likely to be close to the extreme values. Additionally, smaller values of  $U_i$  ( $U$  for a sub-optimal arm  $i$ ), which means it is less likely to draw samples close to the extreme values, reduce the number of selecting a sub-optimal arm  $i$ , thus enhancing overall performance. For our task, as is shown in Figure 3, the values for  $L_{i^*}$  are higher than 1 and  $U_i$  less than 10 in most cases, yielding high empirical performance. We compare the number of pulls observed in our experiments with the expected values based on our theoretical analysis in Appendix E.2, showing that our analysis is not loose.

However, it is essential to note that, in general, finding the optimal arm is challenging if  $\Delta_i$  is close to zero or  $L_{i^*}$  is very small. We assess the performance of MaxUCB on synthetic tasks in Appendix E.4, showing that the performance of MaxUCB deteriorates if the characteristics deviate from our assumptions.

Finally, we provide a regret upper bound that combines the decomposition in Proposition 4.1 with the individual upper bounds above. Indeed, this requires finding a parameter  $\alpha$  that resolves a trade-off between the arms and minimizes the total upper bound. This is done in Corollary 4.3, whose proof is immediate.

**Corollary 4.3.** *If  $L_{i^*}$ ,  $\min_{i \neq i^*}(\Delta_i)$  and  $T$  are known in advance, the exploration parameter  $\alpha$  can be chosen as:*

$$\alpha = \frac{1}{4L_{i^*} \sqrt{\min_{i \neq i^*} \Delta_i}} \left( 1 - \frac{2 \log(\log(T))}{\log(T)} \right). \quad (9)$$

Then, the total regret is bounded by:

$$R(T) \leq \mathcal{O} \left( \frac{K \log T}{\sqrt{T}} \max_{i \leq K} b_i \right). \quad (10)$$

This final result helps to understand the role of  $\alpha$  and serves as guidelines to choose it in practice. Specifically, Equation 9 shows that either a small value of  $L_{i^*}$  or a small sub-optimality gap requires a higher value for  $\alpha$ . Intuitively, a small  $L_{i^*}$  means that the max value of the best arm needs more samples to be nearly reached, and a small suboptimality gap means that the two best arms are close and so hard to distinguish. Indeed, these problem-dependent quantities are unknown to the practitioner, so a direct approach to calculate  $\alpha$  is not feasible. Therefore, evaluating performance robustness under "loose tuning" of  $\alpha$  is essential.

## 5 Performance on AutoML tasks

Next, we examine the empirical performance of MaxUCB in an AutoML setting via reporting average ranking and the number of wins, ties, and losses across tasks for each benchmark (details in Appendix D.1). We first focus on the impact of the hyperparameter  $\alpha$  and then compare our approach to others. Specifically, we show that our two-level approach performs better than single-level HPO on the joint space, and MaxUCB outperforms other state-of-the-art bandit methods. To begin, we will provide a brief overview of the experimental setup used across all experiments.

**Experimental setup.** We use four AutoML benchmarks<sup>4</sup>, all implementing CASH for tabular supervised learning differing in the considered ML models, HPO method, and datasets, which we detail in Table D.1.

For TabRepo and Reshuffling, we use available pre-computed HPO trajectories, whereas for TabRepoRaw and YaHPOGym, we use SMAC [Hutter et al., 2011, Lindauer et al., 2022] as Bayesian optimization method to run HPO ourselves.

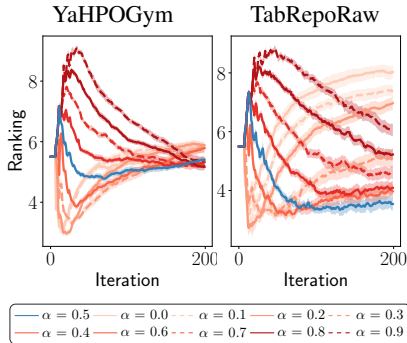


Figure 5: The sensitivity of MaxUCB to hyperparameter  $\alpha$ , lower is better.

**How sensitive is MaxUCB to the choice of  $\alpha$ ?** We study sensitivity to  $\alpha$  in Figure 5, showing that the choice of  $\alpha$  impacts performance. Lower values of  $\alpha$  (light red lines) lead to good performance with small budgets, whereas higher values (dark red lines) achieve stronger final performance when sufficient time is available. An  $\alpha$  around 0.5 yields a balanced trade-off, offering robust anytime performance across tasks (see Appendix D.4 for detailed results). This analysis also indicates the possibility of improving performance by meta-learning how to set  $\alpha$  for a new dataset based on its characteristics and the available time budget. In particular,  $\alpha = 0.5$  is recommended when the reward distribution support is  $[0, 1]$ .

**Competitive Baselines.**

We compare against *Quantile Bayes UCB* [Balef et al., 2024], *ER-UCB-S* [Hu et al., 2021] and *Rising Bandits* [Li et al., 2020] which have been developed for the decomposed CASH task. We consider extreme bandits (*QoMax-SDA* [Baudry et al., 2022], *Max-Median* [Bhatt et al., 2022]) and classic *UCB* as general bandit methods. We use default hyperparameter settings for all methods. As *combined search* baselines, we consider Bayesian optimization (*SMAC*) and *random search*.<sup>5</sup> Additionally, we report the performance of the best (oracle) arm.

**How does the two-level approach compare against *combined search*?** We first compare the average rank over time in Figure 6 using *combined search* (black lines; *random search* and *SMAC* if available) to the two-level approach. We observe that all methods outperform *random search* (dotted line) and that while *SMAC* quickly catches up, some bandit methods continuously achieve a better (lower) rank. Additionally, we observe that any of the mentioned MAB algorithms (except *Rising Bandits* and *QoMax-SDA*) leads to superior performance in the early stages ( $T = 50$ ). This demonstrates that the decomposition is particularly useful when the number of iterations is limited. Additionally, Table 1 shows that the difference in final performance between *combined search* and the two-level approach is significant.

**How does MaxUCB compare against other bandit methods?** Figure 6 shows a substantial difference in the ranking.

In the beginning, many methods perform competitively, but MaxUCB yields the best anytime and final performance. Concretely, classical *UCB* (red) and extreme bandits (*QoMax-SDA*; brown) perform worst. The *Max-Median* algorithm (purple) shows strong initial performance, but its effectiveness declines with more iterations. While *Max-Median* identifies and avoids the worst arm; it sometimes struggles to select the optimal arm, resulting in non-robust performance.

Next, we look at methods that were originally designed for AutoML. Both *ER-UCB-S* (pink) and *Quantile Bayes UCB* (orange) focus on estimating the higher region of the reward distribution rather than the extreme values. *ER-UCB-S* assumes a Gaussian reward distribution and is consistently outperformed by *Quantile Bayes UCB*, a distribution-free algorithm. *Rising Bandits* (green) underperforms initially (requiring  $KC$  steps, where  $K$  is #arms, and  $C$  is a hyperparameter set to 7) but reaches a competitive final performance.

<sup>4</sup>We used the AutoML Toolkit (AMLTK) [Bergman et al., 2024]. We ran HPO on a compute cluster equipped with Intel Xeon Gold 6 240 CPUs, requiring 20 000 CPU hours. We conducted the remaining experiments on a local machine with Intel Core i7-1370P, requiring an additional 32 CPU hours.

<sup>5</sup>Only available for TabRepoRaw and YaHPOGym, where we computed HPO trajectories ourselves.

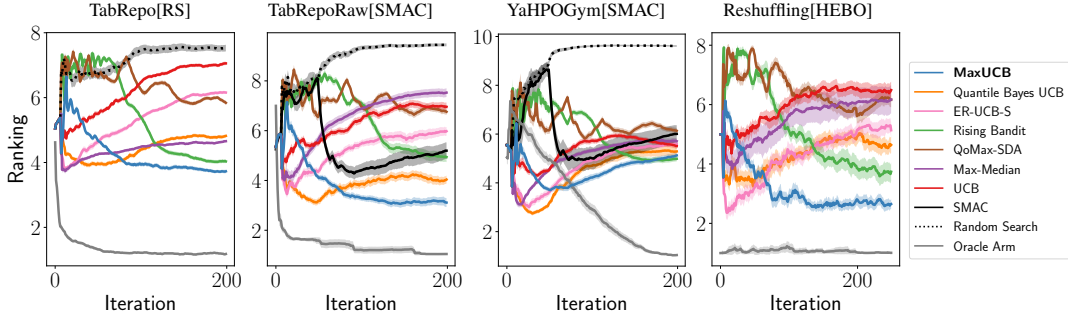


Figure 6: Average rank of algorithms on different benchmarks, lower is better. *SMAC* and *random search* perform *combined search* across the joint space.

Benchmark		MaxUCB	Quantile Bayes UCB	ER-UCB-S	Rising Bandit	QoMax-SDA	Max-Median	UCB
TabRepo [RS]	p-value	<b>0.00000</b>	<b>0.00000</b>	<b>0.00000</b>	<b>0.00000</b>	<b>0.00000</b>	<b>0.00006</b>	<b>0.00000</b>
	w/t/l	186/4/10	179/6/15	135/5/60	185/4/11	172/5/23	126/3/71	135/5/60
TabRepoRaw [SMAC]	p-value	<b>0.00072</b>	<b>0.00261</b>	0.95063	0.42777	0.99194	0.99984	0.99194
	w/t/l	24/0/6	23/0/7	11/0/19	16/0/14	9/0/21	6/0/24	9/0/21
YaHPOGym [SMAC]	p-value	<b>0.00880</b>	<b>0.00503</b>	0.31038	<b>0.00074</b>	0.08372	0.50000	<b>0.02412</b>
	w/t/l	64/0/39	65/0/38	54/1/48	68/0/35	59/0/44	52/0/51	62/0/41

Table 1: P-values from a sign test assessing whether bandit methods outperform *combined search*. P-values below  $\alpha = 0.05$  are underlined, while those below  $\alpha = 0.05$  after multiple comparison correction (adjusting  $\alpha$  by #comparisons) are boldfaced, indicating that the two-level approach is superior to *combined search*. Additionally, we report the number of wins, ties, and losses (w/t/l).

This is especially pronounced for the YaHPOGym benchmark, where *Rising Bandits* outperforms MaxUCB with respect to normalized average performance (see Figure D.5 in Appendix D.5). This benchmark contains datasets where the optimal arm changes over time. Since *Rising Bandits* considers non-stationarity, it performs better for these instances.<sup>6</sup>

Finally, MaxUCB and *Quantile Bayes UCB* are the only ones that significantly outperform *combined search* in Table 1. And looking at TabRepoRaw and Reshuffling, as depicted in Figure 6, demonstrates that MaxUCB is a robust method for CASH problems.

## 6 Discussion and Future Work

This paper addresses the CASH problem, proposing MaxUCB, an MKB method. Our data-driven analysis answers an open question on the applicability of extreme bandits to CASH. We provide a novel theoretical analysis and show state-of-the-art performance on several important benchmarks.

**Limitations.** Though our method can be applied beyond AutoML in principle, it is finely tuned for this setting with bounded and skewed distributions and for maximal value optimization. Our analysis relies on stationary distributions, which might not always be accurate, especially at the beginning of the HPO run, so a short burn-in phase may be needed to reach this regime. Lastly, we provide a default value for our hyperparameter  $\alpha$  that might need adjusting for other applications.

**Impact on AutoML systems.** Our approach complements prior work on AutoML systems and increases their flexibility. Firstly, using a combined search with a single HPO process for CASH may restrict the choice of HPO methods. Thus, a decomposed approach allows to easily integrate recent progress in HPO methods for some ML model classes, e.g., multi-fidelity or meta-learned methods [Li et al., 2018, Falkner et al., 2018, Müller et al., 2023, Chen et al., 2022]. Secondly, some AutoML systems [Swearingen et al., 2017, Li et al., 2023] decompose the search space into smaller subspaces to scale to a distributed setting and use Bandit methods to select promising subspaces [Levine et al.,

<sup>6</sup>A burn-in phase, i.e., pulling each arm for a few rounds at the beginning without observing the rewards, yields a competitive solution as we assess in Appendix E.3.

2017, Li et al., 2020]. While we focus on applying bandits to select promising ML models, our methods could also be applied in this setting.

Moreover, MaxUCB’s application extends beyond the CASH problem. For example, MaxUCB is well-suited for sub-supernet selection in Neural Architecture Search (NAS) [Hu et al., 2022], where we observe similar reward distributions [Ly-Manson et al., 2024] (see Appendix E.5).

**Choosing  $\alpha$  adaptively.** Figure 5 suggests that one could try to tune  $\alpha$  online. However, it is known that, in theory, without additional information, data-adaptive parameters cannot be found at a reasonable exploration cost in bandit optimization settings [Locatelli and Carpentier, 2018]. In AutoML systems, though, supplementary data, like estimates of the sub-optimality gap, reward distribution shape, and HPO convergence rate, can help adjust  $\alpha$  adaptively.

**Future Directions.** Future research could explore leveraging trends in reward sequences, which may reveal valuable patterns, especially in non-stationary settings like AutoML for data streams, where optimal models shift with data distributions [Verma et al., 2024]. Incorporating cost-aware optimization is another promising direction, as computational resources and time, rather than iteration counts, often define budgets in AutoML; this would require estimating model training times and factoring them into the decision process. Addressing the growing complexity of heterogeneous ML tasks, such as those involving pre-training, fine-tuning, or prompt engineering, may benefit from a hierarchical approach that allocates resources effectively across diverse pipelines. Additionally, exploiting structural similarities among algorithms and their hyperparameters could reduce exploration costs by sharing information across arms in the CASH problem, further enhancing efficiency.

## References

- F. Hutter, L. Kotthoff, and J. Vanschoren, editors. *Automated Machine Learning: Methods, Systems, Challenges*. Springer, 2019. Available for free at <http://automl.org/book>.
- M. Baratchi, C. Wang, S. Limmer, J. van Rijn, H. Hoos, B. Thomas, and M. Olhofer. Automated machine learning: past, present and future. *Artificial Intelligence Review*, 57, 2024.
- C. Thornton, F. Hutter, H. Hoos, and K. Leyton-Brown. Auto-WEKA: combined selection and Hyperparameter Optimization of classification algorithms. In I. Dhillon, Y. Koren, R. Ghani, T. Senator, P. Bradley, R. Parekh, J. He, R. Grossman, and R. Uthurusamy, editors, *The 19th ACM SIGKDD International Conference on Knowledge Discovery and Data Mining (KDD’13)*, pages 847–855. ACM Press, 2013.
- Boris van Breugel and Mihaela van der Schaar. Why tabular foundation models should be a research priority. In Salakhutdinov et al. [2024].
- A. Kadra, M. Lindauer, F. Hutter, and J. Grabocka. Well-tuned simple nets excel on tabular datasets. In Ranzato et al. [2021].
- Y. Gorishniy, I. Rubachev, V. Khrulkov, and A. Babenko. Revisiting deep learning models for tabular data. In Ranzato et al. [2021].
- Y. Gorishniy, I. Rubachev, N. Kartashev, D. Shlenskii, A. Kotelnikov, and A. Babenko. TabR: Tabular deep learning meets nearest neighbors. In *International Conference on Learning Representations (ICLR’24)*, 2024. Published online: [iclr.cc](https://arxiv.org/abs/2402.02700).
- D. McElfresh, S. Khandagale, J. Valverde, V. Prasad, B. Feuer, C. Hegde, G. Ramakrishnan, M. Goldblum, and C. White. When do neural nets outperform boosted trees on tabular data? In E. Denton, J. Ha, and J. Vanschoren, editors, *Proceedings of the Neural Information Processing Systems Track on Datasets and Benchmarks*, 2023.
- Ravin Kohli, Matthias Feurer, Katharina Eggensperger, Bernd Bischl, and Frank Hutter. Towards quantifying the effect of datasets for benchmarking: A look at tabular machine learning. *Data-centric Machine Learning Research (DMLR) Workshop at ICLR*, 2024.
- N. Hollmann, S. Müller, K. Eggensperger, and F. Hutter. TabPFN: A transformer that solves small tabular classification problems in a second. In *International Conference on Learning Representations (ICLR’23)*, 2023. Published online: [iclr.cc](https://arxiv.org/abs/2302.00977).

- D. Holzmüller, L. Grinsztajn, and I. Steinwart. Better by default: Strong pre-tuned mlps and boosted trees on tabular data. In L. Mackey, A. Globerson, D. Belgrave, J. Tomczak, U. Paquet, and A. Fan, editors, *Proceedings of the 38th International Conference on Advances in Neural Information Processing Systems (NeurIPS'24)*. Curran Associates, 2024.
- M. Feurer, A. Klein, K. Eggenberger, J. Springenberg, M. Blum, and F. Hutter. Efficient and robust automated machine learning. In C. Cortes, N. Lawrence, D. Lee, M. Sugiyama, and R. Garnett, editors, *Proceedings of the 29th International Conference on Advances in Neural Information Processing Systems (NeurIPS'15)*, pages 2962–2970. Curran Associates, 2015.
- B. Komer, J. Bergstra, and C. Eliasmith. Hyperopt-sklearn: Automatic hyperparameter configuration for scikit-learn. In F. Hutter, R. Caruana, R. Bardenet, M. Bilenko, I. Guyon, B. Kégl, and H. Larochelle, editors, *ICML workshop on Automated Machine Learning (AutoML workshop 2014)*, 2014.
- Lars Kotthoff, Chris Thornton, Holger H Hoos, Frank Hutter, and Kevin Leyton-Brown. Auto-WEKA 2.0: Automatic model selection and hyperparameter optimization in WEKA. *Journal of Machine Learning Research*, 18(25):1–5, 2017.
- M. Feurer, K. Eggenberger, S. Falkner, M. Lindauer, and F. Hutter. Auto-Sklearn 2.0: Hands-free automl via meta-learning. *Journal of Machine Learning Research*, 23(261):1–61, 2022.
- Tor Lattimore and Csaba Szepesvári. *Bandit Algorithms*. Cambridge University Press, 2020.
- Matthew Hoffman, Bobak Shahriari, and Nando Freitas. On correlation and budget constraints in model-based bandit optimization with application to automatic machine learning. In *Artificial Intelligence and Statistics*, pages 365–374. PMLR, 2014.
- Sijia Liu, Parikshit Ram, Deepak Vijaykeerthy, Djallel Bouneffouf, Gregory Bramble, Horst Samulowitz, Dakuo Wang, Andrew R. Conn, and Alexander G. Gray. An ADMM based framework for AutoML pipeline configuration. In *AAAI Conference on Artificial Intelligence*, 2019.
- Alexandra Carpentier and Michal Valko. Extreme bandits. In Z. Ghahramani, M. Welling, C. Cortes, N. Lawrence, and K. Weinberger, editors, *Proceedings of the 28th International Conference on Advances in Neural Information Processing Systems (NeurIPS'14)*. Curran Associates, 2014.
- Mastane Achab, Stephan Cléménçon, Aurélien Garivier, Anne Sabourin, and Claire Vernade. *Max K-Armed Bandit: On the ExtremeHunter Algorithm and Beyond*, page 389–404. Springer International Publishing, 2017. ISBN 9783319712468. doi: 10.1007/978-3-319-71246-8\_24. URL [http://dx.doi.org/10.1007/978-3-319-71246-8\\_24](http://dx.doi.org/10.1007/978-3-319-71246-8_24).
- Dorian Baudry, Yoan Russac, and Emilie Kaufmann. Efficient algorithms for extreme bandits. In *International Conference on Artificial Intelligence and Statistics*, 2022.
- Y. Hu, X. Liu, and S. Liand Y. Yu. Cascaded algorithm selection with extreme-region UCB bandit. *IEEE Transactions on Pattern Analysis and Machine Intelligence*, 44(10):6782–6794, 2021.
- Amir Rezaei Balef, Claire Vernade, and Katharina Eggenberger. Towards bandit-based optimization for automated machine learning. In *5th Workshop on practical ML for limited/low resource settings*, 2024. URL <https://openreview.net/forum?id=S5da3rzyuk>.
- Robert Nishihara, David Lopez-Paz, and Léon Bottou. No regret bound for extreme bandits. In *Artificial Intelligence and Statistics*, pages 259–267. PMLR, 2016.
- S. Raschka. Model evaluation, model selection, and algorithm selection in machine learning. *ArXiv*, abs/1811.12808, 2018.
- D. Jones, M. Schonlau, and W. Welch. Efficient global optimization of expensive black box functions. *Journal of Global Optimization*, 13:455–492, 1998.
- R. Garnett. *Bayesian Optimization*. Cambridge University Press, 2022. Available for free at <https://bayesoptbook.com/>.

- J. Snoek, H. Larochelle, and R. Adams. Practical Bayesian optimization of machine learning algorithms. In P. Bartlett, F. Pereira, C. Burges, L. Bottou, and K. Weinberger, editors, *Proceedings of the 26th International Conference on Advances in Neural Information Processing Systems (NeurIPS'12)*, pages 2960–2968. Curran Associates, 2012.
- Y. Chen, A. Huang, Z. Wang, I. Antonoglou, J. Schrittwieser, D. Silver, and N. de Freitas. Bayesian optimization in alphago. *arXiv:1812.06855 [cs.LG]*, 2018.
- A. Cowen-Rivers, W. Lyu, R. Tutunov, Z. Wang, A. Grosnit, R. Griffiths, A. Maraval, H. Jianye, J. Wang, J. Peters, and H. Ammar. HEBO: Pushing the limits of sample-efficient hyper-parameter optimisation. *Journal of Artificial Intelligence Research*, 74:1269–1349, 2022.
- V. Cicerello and S. Smith. The max K-armed bandit: a new model of exploration applied to search heuristic selection. In M. Veloso and S. Kambhampati, editors, *Proceedings of the 20th National Conference on Artificial Intelligence (AAAI'05)*, page 1355–1361. AAAI Press, 2005.
- Matthew J. Streeter and Stephen F. Smith. An asymptotically optimal algorithm for the Max k-Armed Bandit problem. In *AAAI Conference on Artificial Intelligence*, 2006a.
- Alberto Maria Metelli, Francesco Trovo, Matteo Pirola, and Marcello Restelli. Stochastic rising bandits. In K. Chaudhuri, S. Jegelka, L. Song, C. Szepesvári, G. Niu, and S. Sabato, editors, *Proceedings of the 39th International Conference on Machine Learning (ICML'22)*, volume 162 of *Proceedings of Machine Learning Research*. PMLR, 2022.
- Y. Li, J. Jiang, J. Gao, Y. Shao, C. Zhang, and B. Cui. Efficient automatic CASH via rising bandits. In F. Rossi, V. Conitzer, and F. Sha, editors, *Proceedings of the Thirty-Fourth Conference on Artificial Intelligence (AAAI'20)*, pages 4763–4771. Association for the Advancement of Artificial Intelligence, AAAI Press, 2020.
- Hoda Heidari, Michael J Kearns, and Aaron Roth. Tight policy regret bounds for improving and decaying bandits. In S. Kambhampati, editor, *Proceedings of the 25th International Joint Conference on Artificial Intelligence (IJCAI'16)*, pages 1562–1570, 2016.
- Marco Mussi, Alessandro Montenegro, Francesco Trovó, Marcello Restelli, and Alberto Maria Metelli. Best arm identification for stochastic rising bandits. In [Salakhutdinov et al. \[2024\]](#).
- Y. Pushak and H. Hoos. Automl loss landscapes. *ACM Transactions on Evolutionary Learning and Optimization*, 2(3):1–30, 2022.
- Xiu Su, Tao Huang, Yanxi Li, Shan You, Fei Wang, Chen Qian, Changshui Zhang, and Chang Xu. Prioritized architecture sampling with monto-carlo tree search. *2021 IEEE/CVF Conference on Computer Vision and Pattern Recognition (CVPR)*, pages 10963–10972, 2021.
- Matthew J. Streeter and Stephen F. Smith. A simple distribution-free approach to the Max k-Armed Bandit problem. In *International Conference on Principles and Practice of Constraint Programming*, 2006b.
- S. Bhatt, P. Li, and G. Samorodnitsky. Extreme bandits using robust statistics. *IEEE Transactions on Information Theory*, 69(3):1761–1776, 2022.
- Peter Auer. Using confidence bounds for exploitation-exploration trade-offs. *Journal of Machine Learning Research*, 3(Nov):397–422, 2002.
- Edward Bergman, Matthias Feurer, Aron Bahram, Amir Rezaei Balef, Lennart Purucker, Sarah Segel, Marius Lindauer, Frank Hutter, and Katharina Eggensperger. AMLTK: A Modular Automl Toolkit in Python. *Journal of Open Source Software*, 9(100):6367, 2024. doi: 10.21105/joss.06367. URL <https://doi.org/10.21105/joss.06367>.
- F. Hutter, H. Hoos, and K. Leyton-Brown. Sequential model-based optimization for general algorithm configuration. In C. Coello, editor, *Proceedings of the Fifth International Conference on Learning and Intelligent Optimization (LION'11)*, volume 6683 of *Lecture Notes in Computer Science*, pages 507–523. Springer, 2011.

- M. Lindauer, K. Eggenberger, M. Feurer, A. Biedenkapp, D. Deng, C. Benjamins, T. Ruhkopf, R. Sass, and F. Hutter. SMAC3: A versatile bayesian optimization package for Hyperparameter Optimization. *Journal of Machine Learning Research*, 23(54):1–9, 2022.
- Lisha Li, Kevin Jamieson, Giulia DeSalvo, Afshin Rostamizadeh, and Ameet Talwalkar. Hyperband: A novel bandit-based approach to hyperparameter optimization. *Journal of Machine Learning Research*, 18(185):1–52, 2018.
- S. Falkner, A. Klein, and F. Hutter. BOHB: Robust and efficient Hyperparameter Optimization at scale. In J. Dy and A. Krause, editors, *Proceedings of the 35th International Conference on Machine Learning (ICML’18)*, volume 80, pages 1437–1446. Proceedings of Machine Learning Research, 2018.
- Samuel G. Müller, Matthias Feurer, Noah Hollmann, and Frank Hutter. PFNs4BO: In-context learning for bayesian optimization. In A. Krause, E. Brunskill, K. Cho, B. Engelhardt, S. Sabato, and J. Scarlett, editors, *Proceedings of the 40th International Conference on Machine Learning (ICML’23)*, volume 202 of *Proceedings of Machine Learning Research*. PMLR, 2023.
- Yutian Chen, Xingyou Song, Chansoo Lee, Zi Wang, Richard Zhang, David Dohan, Kazuya Kawakami, Greg Kochanski, Arnaud Doucet, Marc’auelio Ranzato, et al. Towards learning universal hyperparameter optimizers with transformers. In S. Koyejo, S. Mohamed, A. Agarwal, D. Belgrave, K. Cho, and A. Oh, editors, *Proceedings of the 36th International Conference on Advances in Neural Information Processing Systems (NeurIPS’22)*, pages 32053–32068. Curran Associates, 2022.
- Thomas Swearingen, Will Drevo, Bennett Cyphers, Alfredo Cuesta-Infante, Arun Ross, and Kalyan Veeramachaneni. ATM: A distributed, collaborative, scalable system for automated machine learning. In *2017 IEEE international conference on big data (big data)*, pages 151–162. IEEE, 2017.
- Yang Li, Yu Shen, Wentao Zhang, Ce Zhang, and Bin Cui. VolcanoML: speeding up end-to-end AutoML via scalable search space decomposition. *The VLDB Journal*, 32(2):389–413, 2023.
- Nir Levine, Koby Crammer, and Shie Mannor. Rotting bandits. In I. Guyon, U. von Luxburg, S. Bengio, H. Wallach, R. Fergus, S. Vishwanathan, and R. Garnett, editors, *Proceedings of the 31st International Conference on Advances in Neural Information Processing Systems (NeurIPS’17)*. Curran Associates, 2017.
- Shoukang Hu, Ruochen Wang, HONG Lanqing, Zhenguo Li, Cho-Jui Hsieh, and Jiashi Feng. Generalizing few-shot NAS with gradient matching. In *International Conference on Learning Representations (ICLR’22)*, 2022.
- Timotée Ly-Manson, Mathieu Leonardon, Abdeldjalil Aissa El Bey, Ghouti Boukli Hacene, and Lukas Mauch. Analyzing few-shot neural architecture search in a metric-driven framework. In [Eggenberger et al. \[2024\]](#).
- Andrea Locatelli and Alexandra Carpentier. Adaptivity to smoothness in X-armed bandits. In *Annual Conference Computational Learning Theory*, 2018.
- Nilesh Verma, Albert Bifet, Bernhard Pfahringer, and Maroua Bahri. ASML: A scalable and efficient AutoML solution for data streams. In [Eggenberger et al. \[2024\]](#).
- R. Salakhutdinov, Z. Kolter, K. Heller, A. Weller, N. Oliver, J. Scarlett, and F. Berkenkamp, editors. *Proceedings of the 41st International Conference on Machine Learning (ICML’24)*, volume 235 of *Proceedings of Machine Learning Research*, 2024. PMLR.
- M. Ranzato, A. Beygelzimer, K. Nguyen, P. Liang, J. Vaughan, and Y. Dauphin, editors. *Proceedings of the 35th International Conference on Advances in Neural Information Processing Systems (NeurIPS’21)*, 2021. Curran Associates.
- K. Eggenberger, R. Garnett, J. Vanschoren, M. Lindauer, and J. Gardner, editors. *Proceedings of the International Conference on Automated Machine Learning (AutoML’24)*, 2024. Proceedings of Machine Learning Research.

- F. Pfisterer, L. Schneider, J. Moosbauer, M. Binder, and B. Bischl. YAHPO Gym – an efficient multi-objective multi-fidelity benchmark for hyperparameter optimization. In I. Guyon, M. Lindauer, M. van der Schaar, F. Hutter, and R. Garnett, editors, *Proceedings of the First International Conference on Automated Machine Learning*. Proceedings of Machine Learning Research, 2022.
- David Salinas and Nick Erickson. TabRepo: A large scale repository of tabular model evaluations and its AutoML applications. In [Eggenberger et al. \[2024\]](#).
- Thomas Nagler, Lennart Schneider, B. Bischl, and Matthias Feurer. Reshuffling resampling splits can improve generalization of hyperparameter optimization. *ArXiv*, abs/2405.15393, 2024.
- Zohar Karnin, Tomer Koren, and Oren Somekh. Almost optimal exploration in multi-armed bandits. In *International Conference on Machine Learning*, pages 1238–1246. PMLR, 2013.
- Nobuaki Kikkawa and Hiroshi Ohno. Materials discovery using Max K-Armed Bandit. *Journal of Machine Learning Research*, 25(100):1–40, 2024.
- J. Demšar. Statistical comparisons of classifiers over multiple data sets. *Journal of Machine Learning Research*, 7:1–30, 2006.
- Peter Auer, Nicolo Cesa-Bianchi, Yoav Freund, and Robert E Schapire. The nonstochastic multiarmed bandit problem. *SIAM journal on computing*, 32(1):48–77, 2002.

## Table of Contents for the Appendices

- **Appendix A: Preliminaries** ..... 16
- **Appendix B: Proofs** ..... 16
  - B.1 Proof of Lemma 3.3 ..... 16
  - B.2 Proof of Proposition 4.1 ..... 17
  - B.3 Proof of Theorem 4.2 ..... 18
- **Appendix C: More Details on Reward Distribution** ..... 21
  - C.1 Reward Distribution Analysis ..... 21
  - C.2 More Details on Lemma 3.3 ..... 22
  - C.3 Empirical Validation of Lemma 3.3 ..... 23
- **Appendix D: More Details on the Experiments** ..... 26
  - D.1 Metric Calculation ..... 26
  - D.2 Experimental Setup ..... 26
  - D.3 Baselines and Their Hyperparameters ..... 30
  - D.4 More Results on the Sensitivity Analysis of Hyperparameter  $\alpha$  ..... 31
  - D.5 More Results for the Empirical Evaluation ..... 34
  - D.6 More Baselines for the Empirical Evaluation ..... 36
- **Appendix E: More Details on the Empirical Behaviour of MaxUCB** ..... 38
  - E.1 The Number of Times Each Arm is Pulled ..... 38
  - E.2 From Theory to Practice ..... 40
  - E.3 Addressing Non-Stationary Rewards ..... 40
  - E.4 Toy Examples from the Extreme Bandit’s Literature ..... 42
  - E.5 Supernet Selection in Few-Shot Neural Architecture Search ..... 44

## A Preliminaries

**Lemma A.1.** Let  $X_1, \dots, X_n$  be  $n$  samples independently drawn from distribution  $d$ , and let  $G(x) = P(X > x)$  be the survival function. We have:

$$\begin{aligned} P\left(\max_{1 \leq t \leq n} X_t \leq x\right) &\leq e^{-nG(x)}, \\ P\left(\max_{1 \leq t \leq n} X_t > x\right) &\leq nG(x). \end{aligned} \quad (11)$$

*Proof.* Let  $F(x) = P(X \leq x)$  be the cumulative distribution function, so  $G(x) = 1 - F(x) = P(X > x)$ . First, consider the probability that the maximum of the  $n$  samples is less than or equal to  $x$ :

$$P\left(\max_{1 \leq t \leq n} X_t \leq x\right) = \prod_{i=1}^n P(X_i \leq x) = (F(x))^n = (1 - G(x))^n \leq e^{-nG(x)}, \quad (12)$$

using the inequality  $(1 - x)^n \leq e^{-nx}$ . Next, consider the probability that the maximum of the  $n$  samples is greater than  $x$ :

$$P\left(\max_{1 \leq t \leq n} X_t > x\right) \leq \sum_{i=1}^n P(X_i > x) = nG(x). \quad (13)$$

□

## B Proofs

### B.1 Proof of Lemma 3.3

**Lemma 3.3.** Suppose Assumption 3.2 holds. Then, there exists  $L, U \geq 0$  such that the survival function  $G$  can be bounded near  $b$  by two linear functions.

$$\forall \epsilon \in (0, b - a), \quad L\epsilon \leq G(b - \epsilon) \leq U\epsilon \quad (14)$$

*Proof.* By applying the Mean Value Theorem (MVT) to the survival function  $G$  over an interval  $[b - \epsilon, b]$ , there exists a point  $c \in (b - \epsilon, b)$  such that:

$$G(b) - G(b - \epsilon) = G'(c)(b - (b - \epsilon)) = G'(c)\epsilon \quad (15)$$

Since  $G'(x) = -f(x)$  where  $f(x)$  the probability density function (PDF) and  $G(b) = 0$  we have:

$$G(b - \epsilon) = f(c)\epsilon \quad (16)$$

Let  $L$  and  $U$  be the minimum and maximum values of the PDF  $f(c) = \frac{G(b-\epsilon)}{\epsilon}$  over  $\epsilon \in (0, b - a)$ .

$$L\epsilon \leq G(b - \epsilon) \leq U\epsilon \quad (17)$$

Notably, in cases where we are interested in the survival function near some  $b_1 < b$  and  $a_1 > a$  i.e., over  $(b_1 - \epsilon, b_1)$  applying the MVT again, there exists  $c \in (b_1 - \epsilon, b_1)$  such that:

$$G(b_1) - G(b_1 - \epsilon) = G'(c)\epsilon = -f(c)\epsilon \quad (18)$$

which rearranges to:

$$G(b_1 - \epsilon) = f(c)\epsilon + G(b_1) \quad (19)$$

For any  $\epsilon \in (\delta, b_1 - a_1)$  with  $\delta > 0$  we can bound  $G(b_1 - \epsilon)$  as:

$$L\epsilon \leq L\epsilon + G(b_1) \leq G(b_1 - \epsilon) \leq \left(f(c) + \frac{G(b_1)}{\delta}\right)\epsilon \leq U\epsilon \quad (20)$$

□

## B.2 Proof of Proposition 4.1

**Proposition 4.1.** (Upper Regret Bound) the upper regret bound up to time  $T$  is related to the number of times sub-optimal arms are pulled,

$$R(T) \leq \frac{\max_{i \leq K} b_i}{T} \sum_{i \neq i^*}^K N_i(T) \quad (21)$$

Where  $N_i(T) = \mathbb{E}(\sum_{t=1}^T \mathbb{1}\{I_t = i\})$  is the number of sub-optimal pulls of arm  $i$ , arm  $i^*$  is the optimal arm and  $b_i$  is the upper bound on the reward of arm  $i$  as given by Assumption 3.2, i.e., the reward of arm  $i$  lies within the interval  $[a_i, b_i]$ .

*Proof.* This proof is inspired by Assumption 1 of [Baudry et al. \[2022\]](#). First, we need to determine an upper bound for the difference in the highest observed reward for arm  $i$  when it has been pulled for  $N_i(T)$  times compared to when it has been pulled for  $T$  times.

$$\begin{aligned} & \mathbb{E} \left[ \max_{t \leq T} r_{i,t} \right] - \mathbb{E} \left[ \max_{t \leq N_i(T)} r_{i,t} \right] = \mathbb{E} \left[ \mathbb{1} \left\{ \max_{N_i(T)+1 \leq t \leq T} r_{i,t} = \max_{t \leq T} r_{i,t} \right\} \max_{N_i(T)+1 \leq t \leq T} r_{i,t} \right] \\ & \leq \mathbb{E} \left[ \mathbb{1} \left\{ \max_{N_i(T)+1 \leq t \leq T} r_{i,t} = \max_{t \leq T} r_{i,t} \right\} \underbrace{\mathbb{1} \left\{ \max_{N_i(T)+1 \leq t \leq T} r_{i,t} \leq B \right\}}_{\leq B} \max_{N_i(T)+1 \leq t \leq T} r_{i,t} \right] \\ & \quad + \mathbb{E} \left[ \mathbb{1} \left\{ \max_{N_i(T)+1 \leq t \leq T} r_{i,t} = \max_{t \leq T} r_{i,t} \right\} \mathbb{1} \left\{ \max_{N_i(T)+1 \leq t \leq T} r_{i,t} > B \right\} \max_{N_i(T)+1 \leq t \leq T} r_{i,t} \right] \\ & \leq P \left( \max_{N_i(T)+1 \leq t \leq T} r_{i,t} = \max_{t \leq T} r_{i,t} \right) B \\ & \quad + \mathbb{E} \left[ \mathbb{1} \left\{ \max_{N_i(T)+1 \leq t \leq T} r_{i,t} = \max_{t \leq T} r_{i,t} \right\} \mathbb{1} \left\{ \max_{N_i(T)+1 \leq t \leq T} r_{i,t} > B \right\} \max_{N_i(T)+1 \leq t \leq T} r_{i,t} \right]. \quad (22) \end{aligned}$$

Since always  $\max_{N_i(T)+1 \leq t \leq T} r_{i,t} \leq b_i$  by choosing  $B = b_i$  we ensure that

$\mathbb{1} \left\{ \max_{N_i(T)+1 \leq t \leq T} r_{i,t} > B \right\} = 0$ , leading to:

$$\begin{aligned} \mathbb{E} \left[ \max_{t \leq T} r_{i,t} \right] - \mathbb{E} \left[ \max_{t \leq N_i(T)} r_{i,t} \right] & \leq P \left( \max_{N_i(T)+1 \leq t \leq T} r_{i,t} = \max_{t \leq T} r_{i,t} \right) B \\ & \leq \left( 1 - \frac{N_i(T)}{T} \right) B = \left( 1 - \frac{N_i(T)}{T} \right) b_i. \quad (23) \end{aligned}$$

Using this and according to the regret definition, we obtain the following:

$$\begin{aligned}
R(T) &= \mathbb{E}[\max_{t \leq T} r_{i^*, t}] - \mathbb{E}[\max_{t \leq T} r_{I_t, t}] \\
&\leq \mathbb{E} \left[ \max_{t \leq T} r_{i^*, t} \right] - \max_{i \leq K} \mathbb{E} \left[ \max_{t \leq N_i(T)} r_{i, t} \right] \\
&= \min_{i \leq K} \left( \mathbb{E} \left[ \max_{t \leq T} r_{i^*, t} \right] - \mathbb{E} \left[ \max_{t \leq N_i(T)} r_{i, t} \right] \right) \\
&= \min_{i \leq K} \left( \Delta_i + \underbrace{\mathbb{E} \left[ \max_{t \leq T} r_{i, t} \right] - \mathbb{E} \left[ \max_{t \leq N_i(T)} r_{i, t} \right]}_{\text{Equation 23}} \right) \\
&\leq \min_{i \leq K} \left( \Delta_i + \left(1 - \frac{N_i(T)}{T}\right) b_i \right) \\
&\leq \min_{i \leq K} \left( \Delta_i + \left(1 - \frac{N_i(T)}{T}\right) \max_{i \leq K} b_i \right) \tag{24}
\end{aligned}$$

Based on Definition 3.1, the suboptimality gap for the optimal arm  $i^*$  is zero ( $\Delta_{i^*} = 0$ ). Additionally, the total number of pulls for the optimal arm  $N_{i^*}(T)$  can be calculated as the difference between the total number of pulls across all arms  $T$  and the pulls for all suboptimal arms ( $i \neq i^*$ ), i.e.

$N_{i^*}(T) = T - \sum_{i \neq i^*}^K N_i(T)$ . We upper bound the min in equation 24 by the specific value for the optimal arm  $i^*$ :

$$R(T) \leq \frac{\max_{i \leq K} b_i}{T} \sum_{i \neq i^*}^K N_i(T) \tag{25}$$

□

### B.3 Proof of Theorem 4.2

**Theorem 4.2.** For any suboptimal arm  $i \neq i^*$ , the number of suboptimal draws  $N_i(T)$  performed by Algorithm 1 up to time  $T$  is bounded by

$$N_i(T) \leq \frac{T^{1-2L_{i^*} \alpha \sqrt{\Delta_i}}}{1 - 2L_{i^*} \alpha \sqrt{\Delta_i}} + 2\alpha \sqrt{U_i T} \log(T) \tag{26}$$

*Proof.* In order to find the upper bound for the number of sub-optimal pulls of arm  $i$  for the algorithm 1, without loss of generality, we assume that arm 1 is the optimal arm, i.e.  $i^* = 1$ . Let  $\Delta_i = \mathbb{E}[\max_{t \leq T} r_{1, t}] - \mathbb{E}[\max_{t \leq T} r_{i, t}]$  be the suboptimality gap. Our goal is to determine an upper bound on  $N_i(T)$ , the number of times the sub-optimal arm  $i$  has been pulled up to time  $T$ . First, we identify the event that the algorithm pulls the sub-optimal arm  $i$  at time  $t$ :

$$\begin{aligned}
S &= \{ \max(r_{1,1}, \dots, r_{1, n_1(t)}) + C_t(n_1(t)) \leq \max(r_{i,1}, \dots, r_{i, n_i(t)}) + C_t(n_i(t)) \} \\
&= \left\{ \max_{1 \leq n \leq n_1(t)} r_{1, n} + C_t(n_1(t)) \leq \max_{1 \leq n \leq n_i(t)} r_{i, n} + C_t(n_i(t)) \right\} \tag{27}
\end{aligned}$$

where  $S$  is the event of selecting a sub-optimal arm  $i$  with a padding function  $C_t(n)$ . The exploration bonus  $C_t(n)$  is a function that is designed to account for the exploration-exploitation trade-off and typically depends on  $t$  and the number of times each arm has been pulled  $n$ . Let  $n_1(t)$  and  $n_i(t)$  represent the number of times the optimal arm 1 and an sub-optimal arm  $i$  have been pulled, respectively, where  $n_1(t) \leq t$  and  $n_i(t) \leq t$ . We want to express  $S$  in a union of events that covers all possible scenarios leading to  $S$ . Thus, we split  $S$  into two complementary conditions as follows:

$$S \subseteq \left\{ \max_{1 \leq n \leq n_1(t)} r_{1, n} + C_t(n_1(t)) \leq x \right\} \cup \left\{ \max_{1 \leq n \leq n_i(t)} r_{i, n} + C_t(n_i(t)) > x \right\} \tag{28}$$

Where  $x$  is a threshold value, we take  $x = \mathbb{E}[\max_{t \leq T} r_{i,t}]$ ,

$$\begin{aligned}
S &\subseteq \left\{ \max_{1 \leq n \leq n_1(t)} r_{1,n} + C_t(n_1(t)) \leq \mathbb{E}[\max_{t \leq T} r_{i,t}] \right\} \\
&\cup \left\{ \max_{1 \leq n \leq n_i(t)} r_{i,n} + C_t(n_i(t)) > \mathbb{E}[\max_{t \leq T} r_{i,t}] \right\} \\
&= \left\{ \max_{1 \leq n \leq n_1(t)} r_{1,n} \leq \mathbb{E}[\max_{t \leq T} r_{1,t}] - \Delta_i - C_t(n_1(t)) \right\} \\
&\cup \left\{ \max_{1 \leq n \leq n_i(t)} r_{i,n} > \mathbb{E}[\max_{t \leq T} r_{i,t}] - C_t(n_i(t)) \right\} \tag{29}
\end{aligned}$$

Thus, the event  $S$  can be contained within the union of two bad events:

- Underestimating the upper confidence bound of extreme values for the optimal arm 1
- Overestimating the upper confidence bound of extreme values for the sub-optimal arm  $i$

Now we use Lemma A.1 to calculate the probability of 29:

$$\begin{aligned}
P(S) &\leq P\left(\left\{ \max_{1 \leq n \leq n_1(t)} r_{1,n} \leq \mathbb{E}[\max_{t \leq T} r_{1,t}] - C_t(n_1(t)) - \Delta_i \right\}\right) \\
&\quad + P\left(\left\{ \max_{1 \leq n \leq n_i(t)} r_{i,n} > \mathbb{E}[\max_{t \leq T} r_{i,t}] - C_t(n_i(t)) \right\}\right) \\
&\leq e^{-n_1(t)G_1\left(\mathbb{E}[\max_{t \leq T} r_{1,t}] - C_t(n_1(t)) - \Delta_i\right)} \\
&\quad + n_i(t)G_i\left(\mathbb{E}[\max_{t \leq T} r_{i,t}] - C_t(n_i(t))\right). \tag{30}
\end{aligned}$$

Now, by applying Lemma 3.3, we can simplify the analysis by eliminating the complexities associated with survival functions  $G_1$  and  $G_i$ .

$$P(S) \leq e^{-n_1(t)L_1(C_t(n_1(t)) + \Delta_i)} + n_i(t)U_iC_t(n_i(t)) \tag{31}$$

For the first term of the right-hand side, by the Arithmetic Mean-Geometric Mean (AM-GM) inequality ( $a + b \geq 2\sqrt{ab}$ ) of equation 31, we have:

$$e^{-n_1(t)L_1(C_t(n_1(t)) + \Delta_i)} \leq e^{-2L_1n_1(t)\sqrt{C_t(n_1(t))\Delta_i}} \tag{32}$$

In this stage, we want to find a proper padding function  $C_t(n)$ , which controls the right-hand side of equation 31 and equation 32. By choosing  $C_t(n) = \left(\frac{\alpha \log(t)}{n}\right)^2$ , we have:

$$e^{-n_1(t)L_1(C_t(n_1(t)) + \Delta_i)} \leq e^{-2L_1n_1(t)\sqrt{C_t(n_1(t))\Delta_i}} = e^{-2L_1\alpha \log(t)\sqrt{\Delta_i}} = t^{-2L_1\alpha\sqrt{\Delta_i}} \tag{33}$$

$$n_i(t)U_iC_t(n_i(t)) \leq \frac{\alpha^2U_i \log^2(t)}{n_i(t)} \tag{34}$$

This selection of the function of extrapolation bonus results in two significant advantages. First, it provides an upper bound for the right-hand side of equation 31 that remains independent of  $n_1$ . Furthermore, equation 32 shows a decreasing trend as the number of pulls for the sub-optimal arm  $i$  increases.

Now, we assume that the sub-optimal arm  $i$  has been played for  $l_i$  times, so  $n_i(t) \geq l_i$ . We want to calculate the number of sub-optimal pulls of arm  $i$  up to time  $T$ :

$$\begin{aligned}
N_i(T) &\leq l_i + \sum_{t=l_i}^T P(S) \leq l_i + \sum_{t=l_i}^T t^{-2L_1\alpha\sqrt{\Delta_i}} + \sum_{t=l_i}^T \frac{\alpha^2U_i \log^2(t)}{l_i} \\
&\leq l_i + \frac{T^{1-2L_1\alpha\sqrt{\Delta_i}}}{1-2L_1\alpha\sqrt{\Delta_i}} + \frac{\alpha^2U_i}{l_i}T \log^2(T) \tag{35}
\end{aligned}$$

By choosing  $l_i = \alpha\sqrt{U_i T} \log(T)$ , we have:

$$N_i(T) \leq \frac{T^{1-2L_1\alpha\sqrt{\Delta_i}}}{1-2L_1\alpha\sqrt{\Delta_i}} + 2\alpha\sqrt{U_i T} \log(T) \quad (36)$$

□

## C More Details on Reward Distribution

### C.1 Reward distribution analysis

In addition to the analysis in the main paper in Figure 2 in Section 3, we collected the output of HPO for all arms upon each model class. We calculate the empirical survival function  $G$  for each dataset and provide the reward distribution analysis for all benchmark tasks.

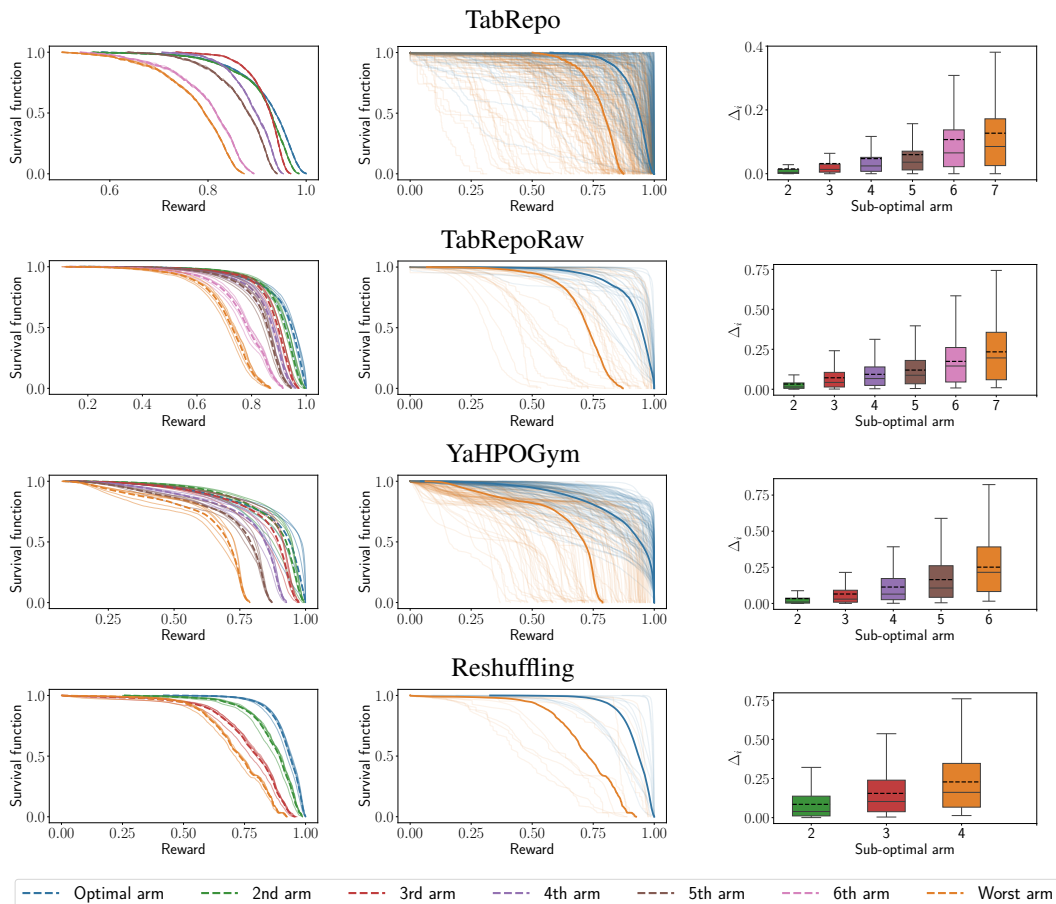


Figure C.1: (Left) The average empirical survival function of rewards (observed performances) per arm ranked per dataset. We divided the reward sequence into five segments over the budget (time horizon) to show the distribution change over time. Thin lines correspond to empirical survival functions for different segments, visualizing the change over time. (Middle) The average empirical survival function per dataset for the best and worst arm with thin lines corresponding to individual datasets. (Right) The sub-optimality gap  $\Delta_i$ .

### C.2 More Details on Lemma 3.3

$L$  and  $U$  are lower and upper bounds for the tangent line approximation of the survival function  $G$  near the maximum value, indicating the shape of the distribution. We provide three examples to demonstrate this numerically.

**Toy example:** Assume two simple survival functions  $G_1(x) = 1 - x^2$  (left skewed, blue curve) and  $G_2(x) = (1 - x)^2$  (right skewed, orange curve) with support  $[0, 1]$ . We calculate  $G(1 - \epsilon)/\epsilon$  over some values of  $\epsilon$  in the Figure C.2. To compute  $L$  and  $U$ , we determine the minimum and maximum values of  $G(1 - \epsilon)/\epsilon$  over the range  $0 < \epsilon < 1$ . For clarity, we restricted  $\epsilon$  to iterate only over the set  $\{0.1, 0.3, 0.5, 0.7, 0.9\}$ . It implies that the calculated values of  $L$  and  $U$  are valid for  $\epsilon \in [0.1, 0.9]$ .

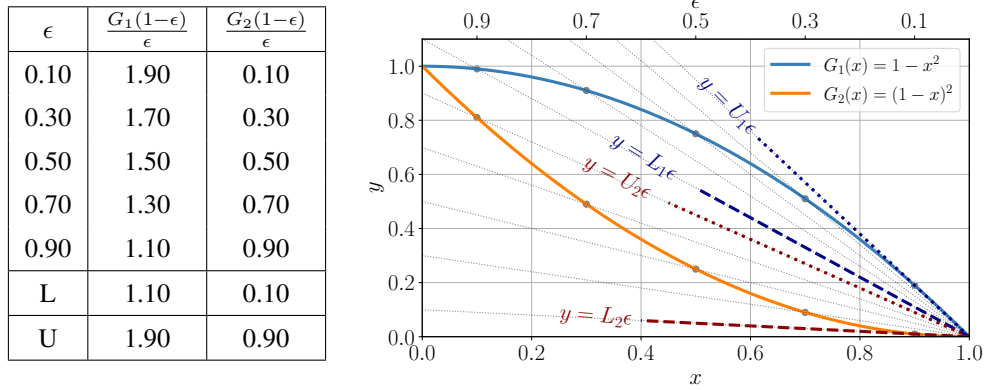


Figure C.2: (Left) Determining  $L$  and  $U$  for  $G_1$  and  $G_2$ . We calculate  $\frac{G(1-\epsilon)}{\epsilon}$  over different ranges of  $\epsilon$ . The minimum and maximum values obtained from this ratio are assigned as  $L$  and  $U$ , respectively. (Right) Showing two survival functions  $G_1$  and  $G_2$  along with their linear line approximations (gray lines). These tangent lines illustrate how  $L$  and  $U$  effectively bound the survival function  $G$  near its maximum value.

**Truncated uniform distribution:** Assume that we have a truncated uniform distribution with support  $[a, b]$ . We know  $G(x) = \frac{b-x}{b-a}$  for  $x \in (a, b)$ . For every  $\epsilon \in [a, b]$  we have  $\frac{G(b-\epsilon)}{\epsilon} = \frac{1}{b-a}$ , which means  $L = U = \frac{1}{b-a}$ .

**Truncated Gaussian distribution:** There is no closed-form solution to formulate  $L$  and  $U$  based on the parameters of the truncated Gaussian distribution. Thus, we show the results of simulations to estimate  $L$  and  $U$  for truncated Gaussian within  $[0, 1]$  with various values  $\mu$  and  $\sigma$ , averaging over 1000 runs in Figure C.3.

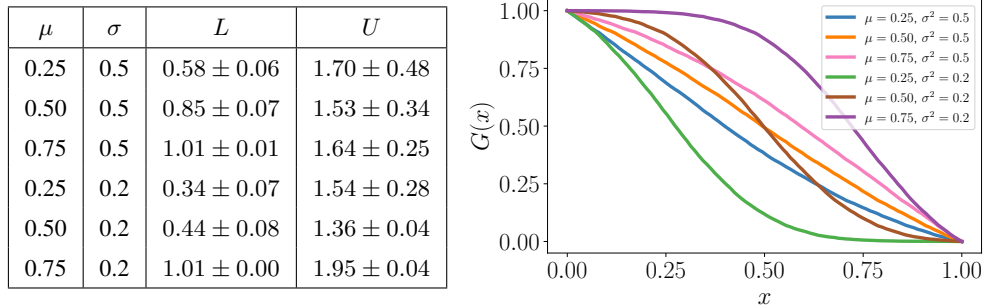


Figure C.3: (Left) Determining  $L$  and  $U$  for truncated Gaussian within  $[0, 1]$  with different values for  $\mu$  and  $\sigma$ . Averaged over 1 000 runs. (Right) Showing survival function of truncated Gaussian distribution with different values for  $\mu$  and  $\sigma$ .

## TabRepo

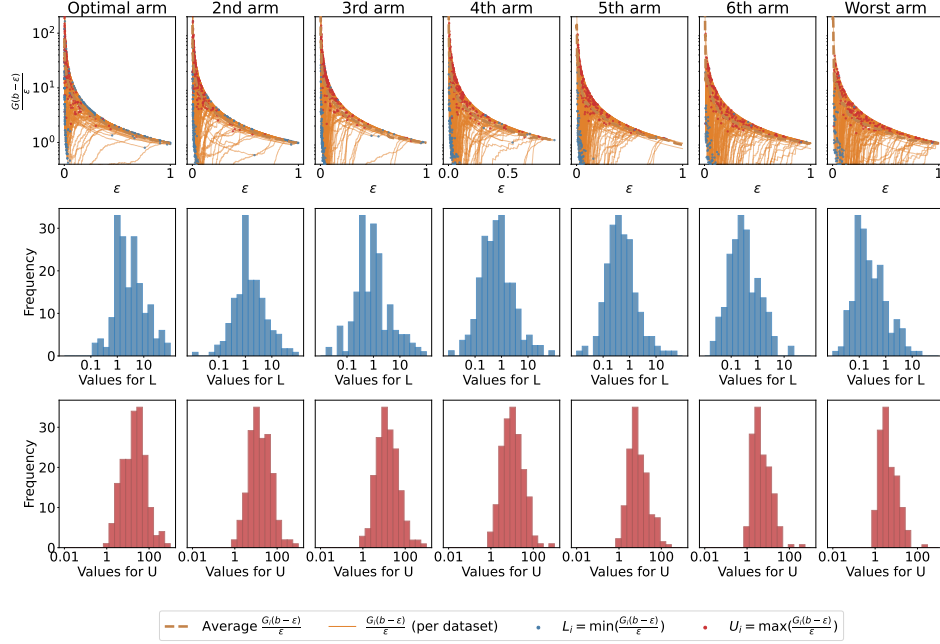


Figure C.4: Arms are ordered by sub-optimality gap. (Top) Thin orange lines represent  $\frac{G(b-\epsilon)}{\epsilon}$ , while the blue and red points correspond to  $L$  and  $U$  for our empirical reward distributions (see Lemma 3.3 for details). (Middle) Histogram of values for  $L$ . (Bottom) Histogram of values for  $U$ .

### C.3 Empirical Validation of Lemma 3.3

To study the empirical values for  $L$  and  $U$  in Lemma 3.3, we leverage the calculated empirical survival function  $G$  for each dataset in Appendix C.1. Specifically, we evaluate  $\frac{G(b-\epsilon)}{\epsilon}$  over the range  $G^{-1}(0.99) < \epsilon < G^{-1}(0.01)$ , where  $G^{-1}(x)$  denotes the inverse of the survival function  $G(x)$ . Focusing on this range allows us to achieve a more robust estimation. Additionally, for TabRepo dataset, we exclude 23 datasets containing an arm with a standard deviation smaller than 0.001, further enhancing the robustness of our analysis. In Figures C.4, C.5, C.6, and C.7, the evaluated values of  $\frac{G(b-\epsilon)}{\epsilon}$  for different benchmarks are shown. Additionally, the values for  $L$  and  $U$ , corresponding to  $\min_{\epsilon}(\frac{G(b-\epsilon)}{\epsilon})$  and  $\max_{\epsilon}(\frac{G(b-\epsilon)}{\epsilon})$ , respectively, are presented. Finally, the histograms of these two variables are also included.

### TabRepoRaw

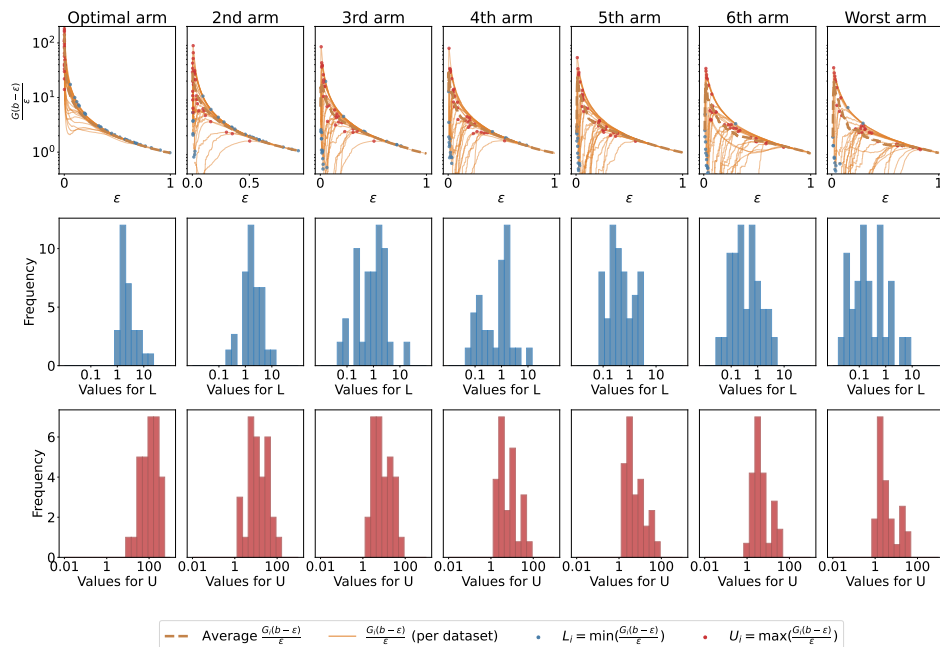


Figure C.5: Arms are ordered by sub-optimality gap. (Top) Thin orange lines represent  $\frac{G(b-\epsilon)}{\epsilon}$ , while the blue and red points correspond to  $L$  and  $U$  for our empirical reward distributions (see Lemma 3.3 for details). (Middle) Histogram of values for  $L$ . (Bottom) Histogram of values for  $U$ .

### YaHPOGym

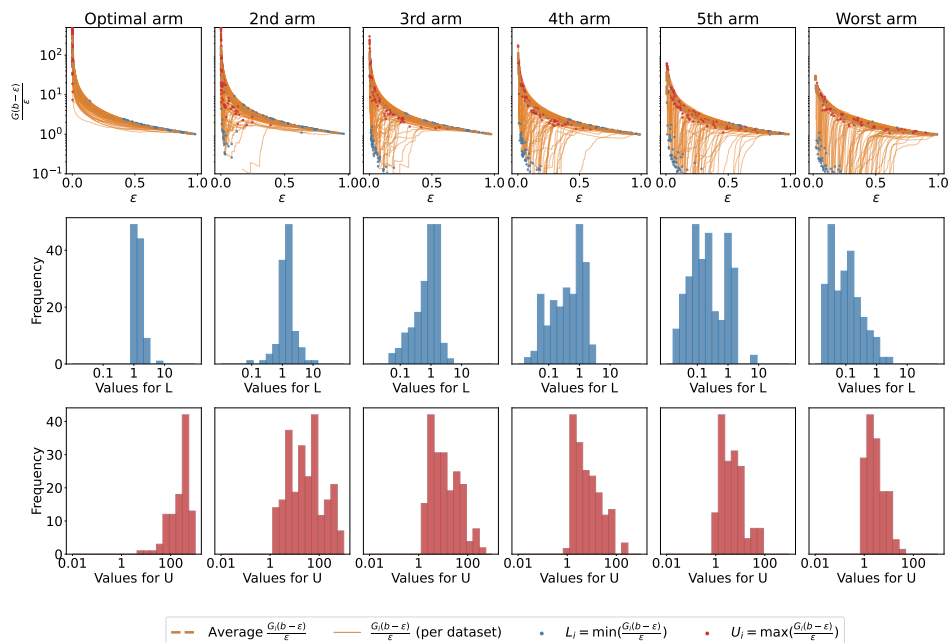


Figure C.6: Arms are ordered by sub-optimality gap. (Top) Thin orange lines represent  $\frac{G(b-\epsilon)}{\epsilon}$ , while the blue and red points correspond to  $L$  and  $U$  for our empirical reward distributions (see Lemma 3.3 for details). (Middle) Histogram of values for  $L$ . (Bottom) Histogram of values for  $U$ .

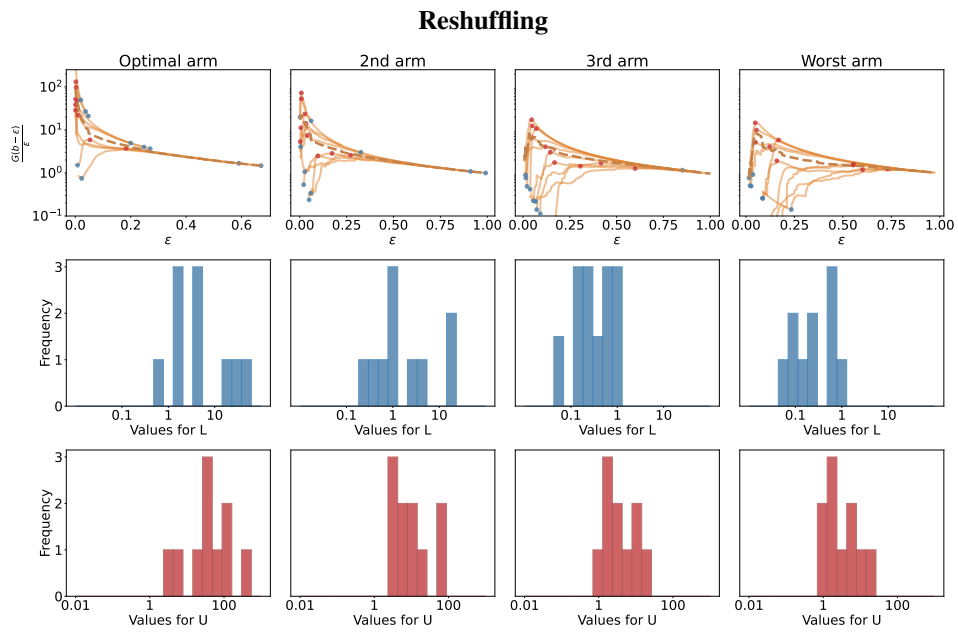


Figure C.7: Arms are ordered by sub-optimality gap. (Top) Thin orange lines represent  $\frac{G(b-\epsilon)}{\epsilon}$ , while the blue and red points correspond to  $L$  and  $U$  for our empirical reward distributions (see Lemma 3.3 for details). (Middle) Histogram of values for  $L$ . (Bottom) Histogram of values for  $U$ .

name	#models	#tasks	type	HPO meth. (rep.)	budget	reference
YaHPOGym	6	103	surrogate	SMAC (32)	200	[Pfisterer et al., 2022]
TabRepo	7	200	tabular	random search (32)	200	[Salinas and Erickson, 2024]
TabRepoRaw	7	30	raw	SMAC (32)	200	-
Reshuffling	4	10	raw	HEBO (30)	250	[Nagler et al., 2024]

Table D.1: Overview of AutoML tasks. For TabRepo and Reshuffling, we use pre-computed HPO trajectories. TabRepoRaw resembles the same model space as TabRepo, but instead of *random search*, we run HPO ourselves. Similarly, we run HPO across provided surrogate HPO benchmark tasks YaHPOGym. We use SMAC [Lindauer et al., 2022, Hutter et al., 2011] implementing Bayesian optimization using Random forests for both tasks.

## D More Details on the Experiments

### D.1 Metric calculation

**Average ranking calculation.** We use bootstrapping with Monte Carlo sampling to calculate the average ranking plot with confidence intervals. For each time step and each task in every dataset, we resample the performance of each repetition (with replacement) and compute the average performance. We then rank the algorithms based on these averaged performances and repeat this process for all tasks. Finally, we average the rankings across tasks. This entire procedure was repeated 1000 times to estimate the confidence interval.

**Number of wins, ties, and losses.** To determine the number of wins, ties, and losses for each task in every dataset, we first compute the average performance of each algorithm over all repetitions at the final time step. We then perform pairwise comparisons of these averaged performances among all algorithms versus *combined search*. To account for negligible differences that are not statistically significant, we consider two performances to be tied if they are sufficiently close. Specifically, we use NumPy’s `isclose` function to compare the averaged performances, treating values within a default tolerance of  $1 \times 10^{-8}$  as equal.

### D.2 Experimental Setup

Here, we provide details on our experimental setups as described in Table D.1.

**YaHPOGym** [Pfisterer et al., 2022], a surrogate benchmark, covers 6 ML models (details in Table D.2) on 103 datasets and uses a regression model (surrogate model) to predict performances for queried hyperparameter settings. We use Bayesian optimization as implemented by SMAC [Lindauer et al., 2022] using Random Forests to conduct HPO. Additionally, we compare our two-level approach to *combined search* using SMAC, SMAC without initial design (SMAC-no-init), and Random Search. We run 32 repetitions and use a budget of 200 iterations for each evaluation.

**TabRepo** [Salinas and Erickson, 2024] consists of pre-evaluated performance scores for 200 iterations of random search for 7 ML models (details in Table D.3) on 200 datasets (context name: *D244\_F3\_C1530\_200*). We run 32 repetitions and use a budget of 200 iterations for each task.

**TabRepoRaw** which uses the search space from TabRepo (details in Table D.3) and allows HPO to evaluate all configurations. For constructing TabRepo [Salinas and Erickson, 2024], each configuration was evaluated with a one-hour time limit and 8-fold cross-validation. To reduce computational requirements for TabRepoRaw, we reduced this to 5 minutes and 4-fold cross-validation, and we provide it for 30 datasets (context name: *D244\_F3\_C1530\_30*). We use Bayesian optimization as implemented by SMAC [Lindauer et al., 2022] using Random Forests to conduct HPO. Additionally, we compare our two-level approach to *combined search* using SMAC, Random Search. We run 32 repetitions and use a budget of 200 iterations for the mentioned task.

To enable a fair comparison, we always evaluate the default configuration for each model first and then allow SMAC to run an initial design of  $50 - \#arms$  configurations in the upper level and  $\frac{50}{\#arms-1}$  in the lower level.

**Reshuffling** [Nagler et al., 2024] which uses Heteroscedastic and Evolutionary Bayesian Optimization solver (HEBO) [Cowen-Rivers et al., 2022] for HPO. This benchmark includes HPO runs for 4 ML

Table D.2: Hyperparameter spaces for ML models in YaHPOGym.

ML model	Hyperparameter	Type	Range	Info
-	trainsize	continuous	[0.03, 1]	=0.525 (fixed)
	imputation	categorical	{mean, median, hist}	=mean (fixed)
Glmnet	alpha	continuous	[0, 1]	log
	s	continuous	[0.001, 1097]	
Rpart	cp	continuous	[0.001, 1]	log
	maxdepth	integer	[1, 30]	
	minbucket	integer	[1, 100]	
	minsplit	integer	[1, 100]	
SVM	kernel	categorical	{linear, polynomial, radial}	log log, kernel log kernel
	cost	continuous	[4.5e-05, 2.2e4]	
	gamma	continuous	[4.5e-05, 2.2e4]	
	tolerance	continuous	[4.5e-05, 2]	
	degree	integer	[2, 5]	
AKNN	k	integer	[1, 50]	log log
	distance	categorical	{l2, cosine, ip}	
	M	integer	[18, 50]	
	ef	integer	[7, 403]	
	ef_construction	integer	[7, 403]	
Ranger	num.trees	integer	[1, 2000]	splitrule
	sample.fraction	continuous	[0.1, 1]	
	mtry.power	integer	[0, 1]	
	respect.unordered.factors	categorical	{ignore, order, partition}	
	min.node.size	integer	[1, 100]	
	splitrule	categorical	{gini, extratrees}	
	num.random.splits	integer	[1, 100]	
XGBoost	booster	categorical	{gblinear, gbtrees, dart}	log log, booster log, booster log log booster log, booster booster booster booster booster
	nrounds	integer	[7, 2980]	
	eta	continuous	[0.001, 1]	
	gamma	continuous	[4.5e-05, 7.4]	
	lambda	continuous	[0.001, 1097]	
	alpha	continuous	[0.001, 1097]	
	subsample	continuous	[0.1, 1]	
	max_depth	integer	[1, 15]	
	min_child_weight	continuous	[2.72, 148.4]	
	colsample_bytree	continuous	[0.01, 1]	
	colsample_bylevel	continuous	[0.01, 1]	
	rate_drop	continuous	[0, 1]	
	skip_drop	continuous	[0, 1]	

models (details in Table D.4) across 10 datasets, with 10 repetitions and 3 different validation split ratios within a budget of 250 iterations. Although the benchmark does not support HPO over the entire search space, it offers a valuable opportunity to compare the performance of bandit methods in a realistic setting.

Table D.3: Hyperparameter spaces for ML models in TabRepo and TabRepoRaw.

ML model	Hyperparameter	Type	Range	Info	Default value
NN(PyTorch)	learning rate	continuous	[1e-4, 3e-2]	log	3e-4
	weight decay	continuous	[1e-12, 0.1]	log	1e-6
	dropout prob	continuous	[0, 0.4]		0.1
	use batchnorm	categorical	False, True		
	num layers	integer	[1, 5]		2
	hidden size	integer	[8, 256]		128
	activation	categorical	relu, elu		
NN(FastAI)	learning rate	continuous	[5e-4, 1e-1]	log	1e-2
	layers	categorical	[200], [400], [200, 100], [400, 200], [800, 400], [200, 100, 50], [400, 200, 100]		
	emb drop	continuous	[0.0, 0.7]		0.1
	ps	continuous	[0.0, 0.7]		0.1
	bs	categorical	256, 128, 512, 1024, 2048		
	epochs	integer	[20, 50]		30
CatBoost	learning rate	continuous	[5e-3, 0.1]	log	0.05
	depth	integer	[4, 8]		6
	l2 leaf reg	continuous	[1, 5]		3
	max ctr complexity	integer	[1, 5]		4
	one hot max size	categorical	2, 3, 5, 10		
	grow policy	categorical	SymmetricTree, Depthwise		
LightGBM	learning rate	continuous	[5e-3, 0.1]	log	0.05
	feature fraction	continuous	[0.4, 1.0]		1.0
	min data in leaf	integer	[2, 60]		20
	num leaves	integer	[16, 255]		31
	extra trees	categorical	False, True		
	XGBoost	learning rate	continuous	[5e-3, 0.1]	log
max depth		integer	[4, 10]		6
min child weight		continuous	[0.5, 1.5]		1.0
colsample bytree		continuous	[0.5, 1.0]		1.0
enable categorical		categorical	False, True		
Extra-trees		max leaf nodes	integer	[5000, 50000]	
	min samples leaf	categorical	1, 2, 3, 4, 5, 10, 20, 40, 80		
	max features	categorical	sqrt, log2, 0.5, 0.75, 1.0		
Random-forest	max leaf nodes	integer	[5000, 50000]		
	min samples leaf	categorical	1, 2, 3, 4, 5, 10, 20, 40, 80		
	max features	categorical	sqrt, log2, 0.5, 0.75, 1.0		

Table D.4: Hyperparameter spaces for ML models in Reshuffling.

ML model	Hyperparameter	Type	Range	Info
Funnel-Shaped MLP	learning rate	continuous	[1e-4, 1e-1]	log
	num layers	integer	[1, 5]	
	max units	categorical	64, 128, 256, 512	
	batch size	categorical.	16, 32, ..., max_batch_size	
	momentum	continuous.	[0.1, 0.99]	
	alpha	continuous.	[1e-6, 1e-1]	log
Elastic Net	C	continuous	[1e-6, 10e4]	log
	l1 ratio	continuous	[0.0, 1.0]	
XGBoost	max depth	integer	[2, 12]	log
	alpha	continuous	[1e-8, 1.5]	log
	lambda	continuous	[1e-8, 1.0]	log
	eta	continuous	[0.01, 0.3]	log
CatBoost	learning rate	continuous	[0.01, 0.3]	log
	depth	integer	[2, 12]	
	l2 leaf reg	continuous	[0.5, 30]	

### D.3 Baselines and their hyperparameters

We use several bandit algorithms as baselines. Table D.5 summarizes the hyperparameters and their values.

Table D.5: Hyperparameters of Bandit Baselines.

Algorithm	Hyperparameter	Value	Reference
MaxUCB	$\alpha$	0.5	Ours
<i>Quantile Bayes UCB</i>	$\alpha$	1.0	Balef et al. [2024]
	$\beta$	0.2	
	$\tau$	0.95	
<i>Quantile UCB</i>	$\alpha$	0.5	
	$\tau$	0.95	
<i>ER-UCB-S</i>	$\beta$	0.6	Hu et al. [2021]
	$\theta$	0.01	
	$\gamma$	20.0	
<i>ER-UCB-N</i>	$\alpha$	1.0	
	$\theta$	0.01	
	$\gamma$	20.0	
<i>Rising Bandits</i>	$C$	7	Li et al. [2020]
	$T$	Time horizon	
<i>Max-Median</i>	$\epsilon$	$1/(t)$ , $t$ is iteration	Bhatt et al. [2022]
<i>QoMax-SDA</i>	$q$	0.5	
	$\gamma$	2/3	
<i>QoMax-ETC</i>	$q$	0.5	Baudry et al. [2022]
	$b_T$	4	
	$n_T$	3	
	$T$	Time horizon	
<i>UCB</i>	$\alpha$	0.5	Auer [2002]
<i>ThresholdAscent</i>	$\delta$	0.1	Streeter and Smith [2006b]
	$s$	20	
	$T$	Time horizon	
<i>Successive Halving</i>	$\eta$	2.0	Karnin et al. [2013]
	$T$	Time horizon	
<i>R-SR</i>	$\epsilon$	0.25	
	$T$	Time horizon	
<i>R-UCBE</i>	$\alpha$	57.12	Mussi et al. [2024]
	$\epsilon$	0.25	
	$\sigma$	0.05	
	$T$	Time horizon	
<i>MaxSearch (Gaussian)</i>	$c$	1.0	Kikkawa and Ohno [2024]
<i>MaxSearch (SubGaussian)</i>	$c$	0.27	

#### D.4 More Results on the Sensitivity Analysis of Hyperparameter $\alpha$

In addition to the results shown in Figure 5 in Section 5, we provide additional results here. We evaluated the performance of MaxUCB for  $\alpha \in [0, 2.9]$  with step size 0.1. We plot the performance over the number of iterations for different values of  $\alpha$  in Figures D.1, D.2, D.3, D.4. Green indicates better performance, showing the impact of  $\alpha$  at different stages of the optimization procedure. Furthermore, we provide a comparison between MaxUCB with different values of  $\alpha$  with *combined search(SMAC)* in Table D.6. For the experiments in the main paper, we choose  $\alpha = 0.5$  as a robust choice over all datasets. Notably,  $\alpha = 0.5$  is selected based on the assumption that the reward distribution support is  $[0, 1]$ . For other supports, we recommend scaling  $\alpha$  according to the range of the support.

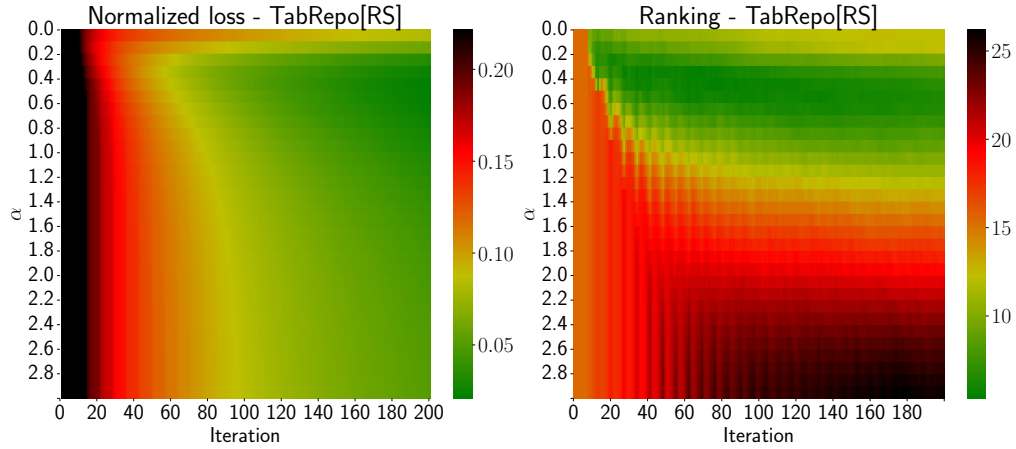


Figure D.1: Heatmap showing the performance of our algorithm with different values of  $\alpha$  for TabRepo dataset.

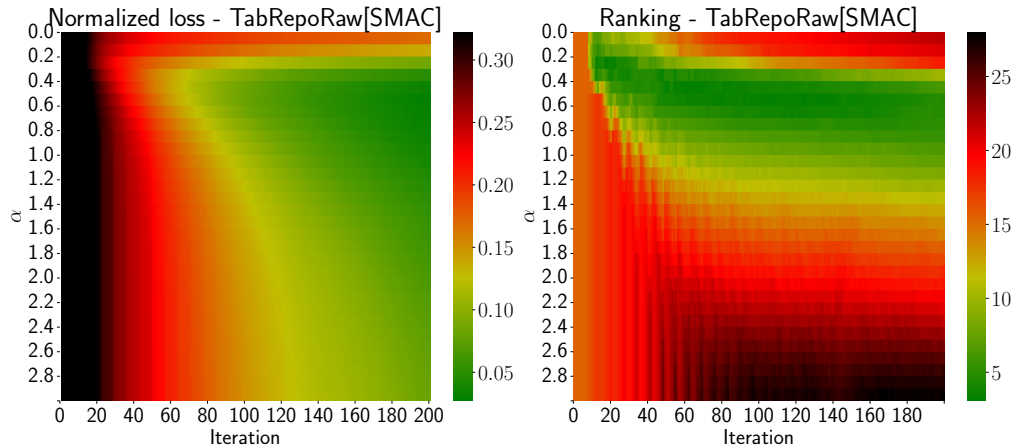


Figure D.2: Heatmap showing the performance of our algorithm with different values of  $\alpha$  for TabRepoRaw dataset.

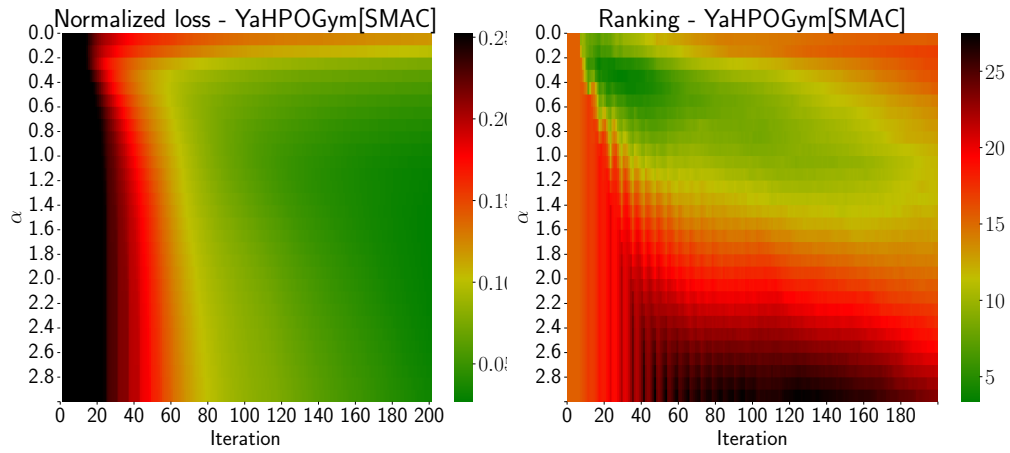


Figure D.3: Heatmap showing the performance of our algorithm with different values of  $\alpha$  for YaHPOGym dataset.

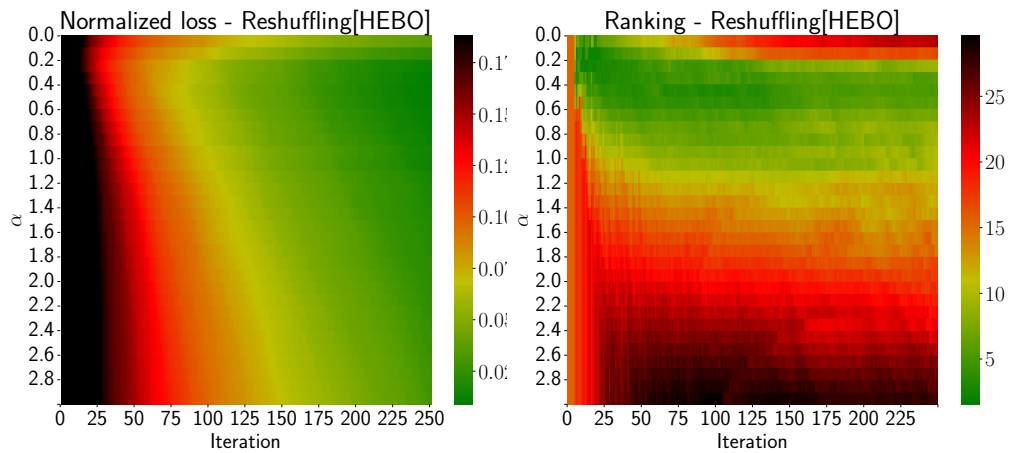


Figure D.4: Heatmap showing the performance of our algorithm with different values of  $\alpha$  for Reshuffling dataset.

Table D.6: Comparing MaxUCB with *combined search(SMAC)* for different values of  $\alpha$  and time steps. P-values from a sign test assessing whether bandit methods outperform *combined search*. P-values below  $\alpha = 0.05$  are underlined, while those below  $\alpha = 0.05$  after multiple comparison correction (adjusting  $\alpha$  by the number of comparisons) are boldfaced and underlined indicating that the two-level approach is superior to *combined search*. Additionally, we report the normalized loss and the number of wins, ties, and losses (w/t/l) of bandit methods.

Time		$\alpha=0.0$	$\alpha=0.1$	$\alpha=0.2$	$\alpha=0.3$	$\alpha=0.4$	$\alpha=0.5$	$\alpha=0.6$	$\alpha=0.7$	$\alpha=0.8$	$\alpha=0.9$	
TabRepoRaw[SMAC]	50	p-value	0.1002	<b><u>0.0214</u></b>	<b><u>0.0000</u></b>							
		w/t/l	19/0/11	21/0/9	27/0/3	29/0/1	29/0/1	29/0/1	29/0/1	28/0/2	27/0/3	27/0/3
		loss	0.2555	0.2446	0.2172	0.1946	0.1965	0.2134	0.2203	0.2229	0.2249	0.2296
	100	p-value	0.9974	0.9919	0.8998	0.1808	<b><u>0.0081</u></b>	<b><u>0.0214</u></b>	0.1002	0.5722	0.8192	0.9919
		w/t/l	8/0/22	9/0/21	12/0/18	18/0/12	22/0/8	21/0/9	19/0/11	15/0/15	13/0/17	9/0/21
		loss	0.2138	0.2053	0.1832	0.1346	0.1283	0.1113	0.1164	0.1208	0.1279	0.1512
	150	p-value	0.9993	0.9919	0.9506	0.2923	<b><u>0.0007</u></b>	<b><u>0.0007</u></b>	<b><u>0.0026</u></b>	<b><u>0.0081</u></b>	0.1002	0.7077
		w/t/l	7/0/23	9/0/21	11/0/19	17/0/13	24/0/6	24/0/6	23/0/7	22/0/8	19/0/11	14/0/16
		loss	0.1994	0.1911	0.1671	0.1020	0.0898	0.0752	0.0775	0.0849	0.0887	0.0973
	200	p-value	0.9998	0.9993	0.9786	0.1808	<b><u>0.0214</u></b>	<b><u>0.0007</u></b>	<b><u>0.0026</u></b>	<b><u>0.0026</u></b>	<b><u>0.0081</u></b>	<b><u>0.0081</u></b>
		w/t/l	6/0/24	7/0/23	10/0/20	18/0/12	21/0/9	24/0/6	23/0/7	23/0/7	22/0/8	22/0/8
		loss	0.1864	0.1790	0.1489	0.0686	0.0651	0.0563	0.0622	0.0698	0.0703	0.0751
YaHPOGym[SMAC]	50	p-value	<b><u>0.0000</u></b>									
		w/t/l	74/1/28	83/1/19	95/1/7	102/1/0	102/1/0	102/1/0	102/1/0	102/1/0	102/1/0	101/1/1
		loss	0.1853	0.1532	0.1071	0.0930	0.0942	0.0978	0.1047	0.1101	0.1151	0.1190
	100	p-value	0.3833	0.3833	0.3833	<b><u>0.0459</u></b>	<b><u>0.0112</u></b>	<b><u>0.0112</u></b>	<b><u>0.0088</u></b>	0.0572	0.2153	0.4220
		w/t/l	53/1/49	53/1/49	53/1/49	60/1/42	63/1/39	63/1/39	64/0/39	60/0/43	56/0/47	53/0/50
		loss	0.1494	0.1177	0.0876	0.0813	0.0782	0.0713	0.0668	0.0702	0.0718	0.0749
	150	p-value	0.3833	0.6167	0.8135	0.0686	<b><u>0.0036</u></b>	<b><u>0.0065</u></b>	<b><u>0.0028</u></b>	<b><u>0.0005</u></b>	<b><u>0.0028</u></b>	<b><u>0.0148</u></b>
		w/t/l	53/1/49	50/1/52	47/1/55	59/1/43	65/1/37	64/1/38	66/0/37	68/1/34	66/0/37	63/0/40
		loss	0.1378	0.1013	0.0758	0.0722	0.0716	0.0551	0.0518	0.0507	0.0520	0.0500
	200	p-value	0.5394	0.8135	0.6896	0.2442	<b><u>0.0185</u></b>	<b><u>0.0088</u></b>	<b><u>0.0015</u></b>	<b><u>0.0002</u></b>	<b><u>0.0000</u></b>	<b><u>0.0001</u></b>
		w/t/l	51/1/51	47/1/55	49/1/53	55/1/47	62/1/40	64/0/39	67/0/36	70/0/33	75/0/28	71/0/32
		loss	0.1190	0.0856	0.0697	0.0660	0.0614	0.0457	0.0443	0.0418	0.0423	0.0421

### D.5 More Results for the Empirical Evaluation

In addition to the analysis in the main paper in Figure 6 in Section 5, we report the averaged normalized loss over time in Figure D.5, the average ranking in Figure D.6, the normalized loss per task in Figure D.7, the ranking per task in Figure D.8 and critical distance plots as described by Demšar [2006] in Figure D.9. Additionally, we report results for a *Random Policy* (yellow) that selects arms to pull at random.

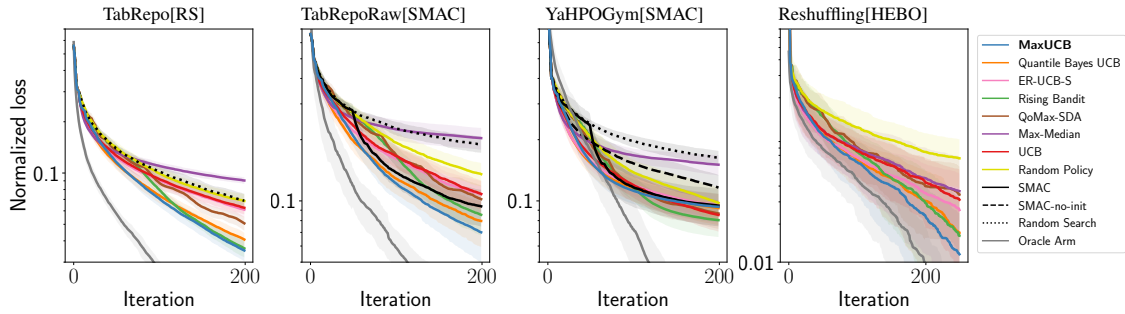


Figure D.5: Average normalized loss of algorithms on different benchmarks, lower is better. *SMAC* and *random search* perform *combined search* across the joint space.

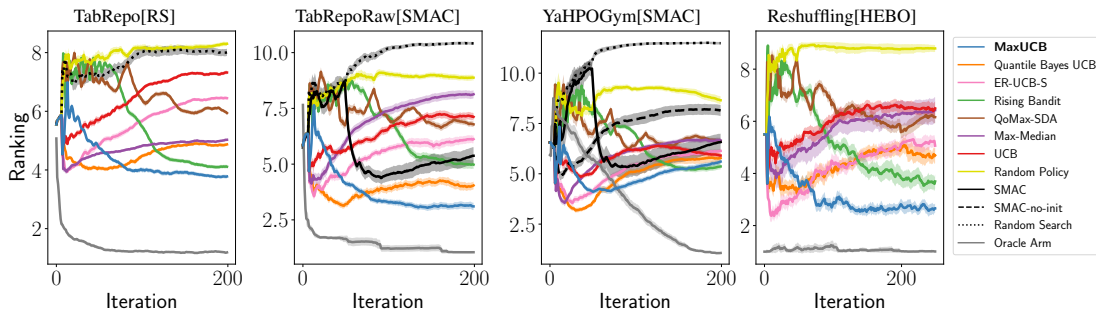


Figure D.6: Average ranking of algorithms on different benchmarks, lower is better. *SMAC* and *random search* perform *combined search* across the joint space.

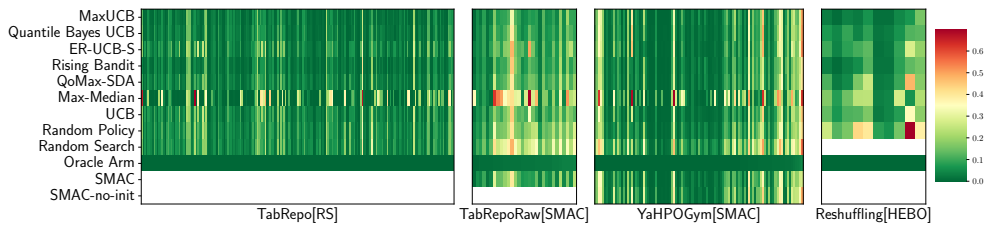


Figure D.7: Heatmap showing the normalized loss of algorithms per task of each benchmark, sorted by the oracle arm performance, lower is better. *SMAC* and *random search* perform *combined search* across the joint space.

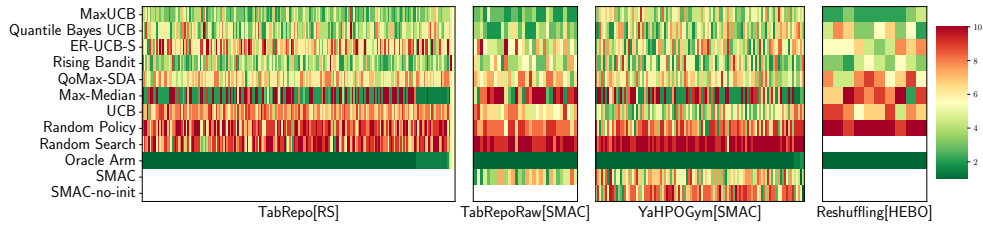


Figure D.8: Heatmap showing the ranking of algorithms per task of each benchmark, sorted by the oracle arm performance, lower is better. *SMAC* and *random search* perform *combined search* across the joint space.

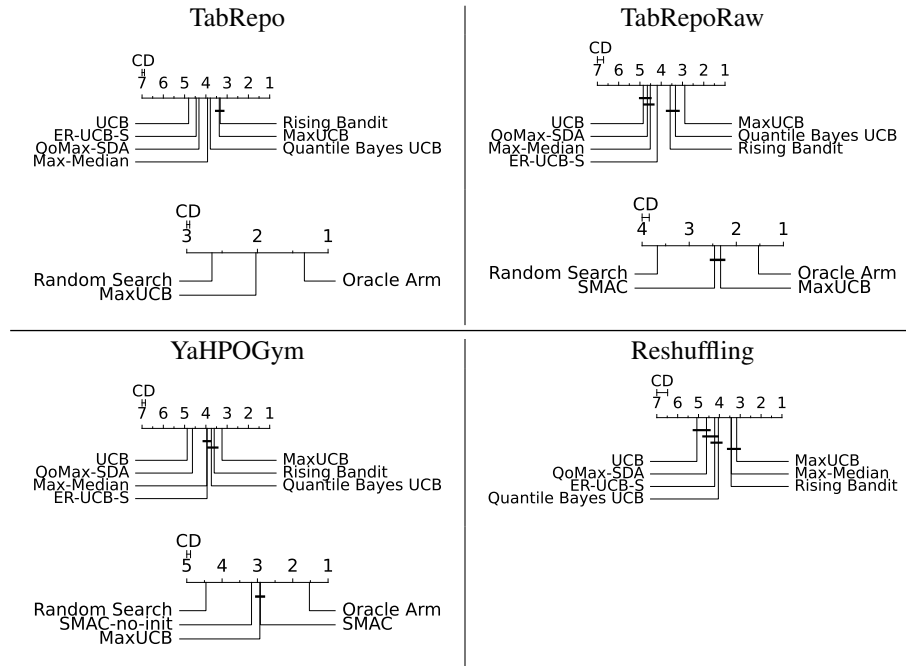


Figure D.9: Diagrams to compare the performance (ranking) of different algorithms using the Critical Distance (CD). For each benchmark on top, we compare bandit methods, and on the bottom, we compare MaxUCB against *combined search* and the oracle arm.

## D.6 More Baselines for the Empirical Evaluation

**Max  $K$ -armed Bandit Baselines.** We compare MaxUCB against *MaxSearch Gaussian* [Kikkawa and Ohno, 2024], *MaxSearch SubGaussian* [Kikkawa and Ohno, 2024], *QoMax-ETC* [Baudry et al., 2022], *QoMax-SDA* [Baudry et al., 2022], *Max-Median* [Bhatt et al., 2022] and *Threshold Ascent* [Streeter and Smith, 2006b]. We report the averaged normalized loss over time in Figure D.10, the average ranking in Figure D.11. As shown, our algorithm outperforms all extreme bandit algorithms in these benchmarks.

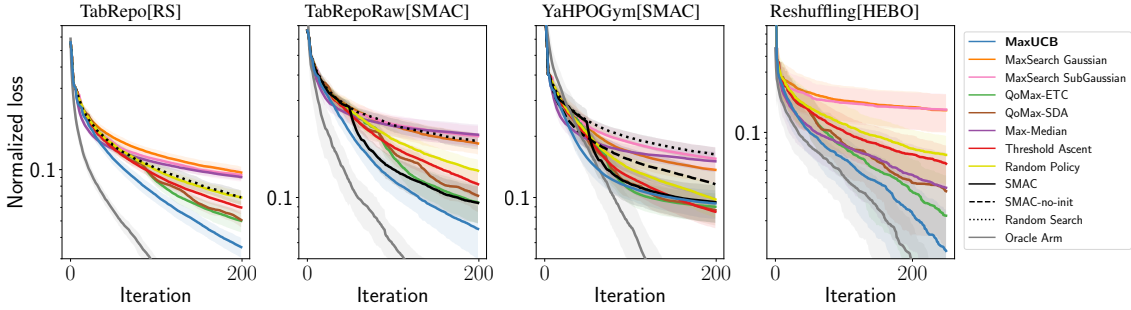


Figure D.10: Average normalized loss of MKB algorithms on different benchmarks, lower is better. *SMAC* and *random search* perform *combined search* across the joint space.

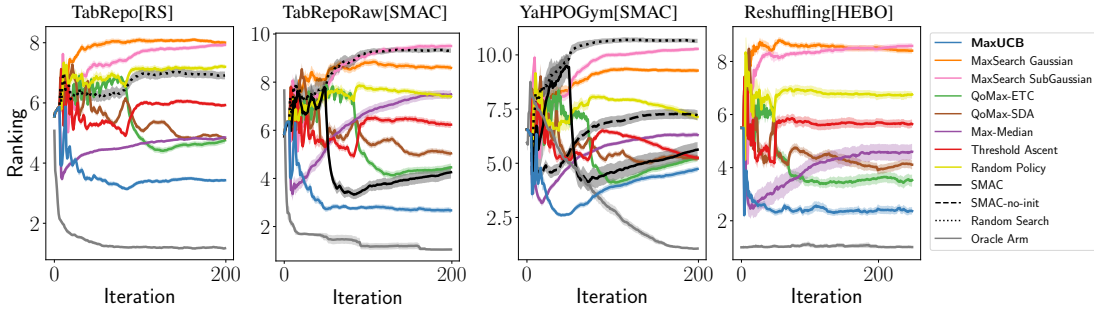


Figure D.11: Average ranking of MKB algorithms on different benchmarks, lower is better. *SMAC* and *random search* perform *combined search* across the joint space.

**A Few More Relevant Bandit Baselines.** We compare MaxUCB against *Quantile UCB* [Balef et al., 2024], *ER-UCB-N* [Hu et al., 2021], *R-SR* [Mussi et al., 2024], *R-UCBE* [Mussi et al., 2024], *Successive Halving* [Karnin et al., 2013] and *EXP3* [Auer et al., 2002]. We report the averaged normalized loss over time in Figure D.12, the average ranking in Figure D.13.

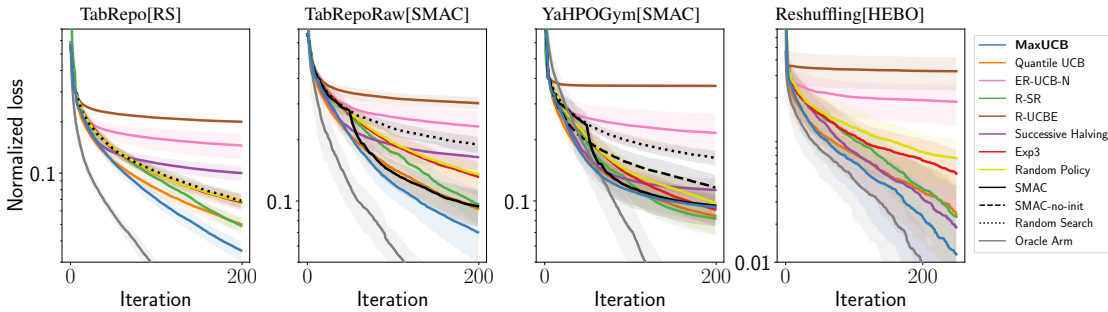


Figure D.12: Average normalized loss of algorithms on different benchmarks, lower is better. *SMAC* and *random search* perform *combined search* across the joint space.

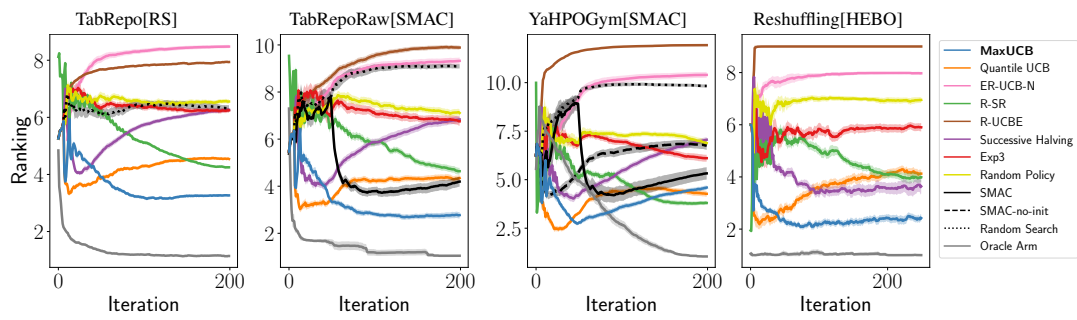


Figure D.13: Average ranking of algorithms on different benchmarks, lower is better. *SMAC* and *random search* perform *combined search* across the joint space.

## E More Details on the Empirical Behaviour of MaxUCB

Here, we provide further analysis of MaxUCB. Concretely, we study how often our algorithm pulls the optimal arm and compare it to the theoretical results. Furthermore, we evaluate an extension of MaxUCB to handle non-stationary rewards and finally study MaxUCB performance on common synthetic benchmarks used in the extreme bandit literature.

### E.1 The number of times each arm is pulled

Proposition 4.1 shows that the number of times the optimal arm is pulled can be viewed as a good metric for measuring the performance of algorithms. Figure E.1, E.2, E.3, E.4 shows the average number of pulling arms on different benchmarks. They indicate that, on average, MaxUCB, *Rising Bandits*, and *Max-Median* algorithms often choose the optimal arm. However, for *Max-Median*, the number of pulls of the optimal arm is either very close to 0 or to  $T$ , leading to a non-robust performance, which has already been observed in Baudry et al. [2022] experiments. *UCB* and *ER-UCB-S* perform almost similarly.

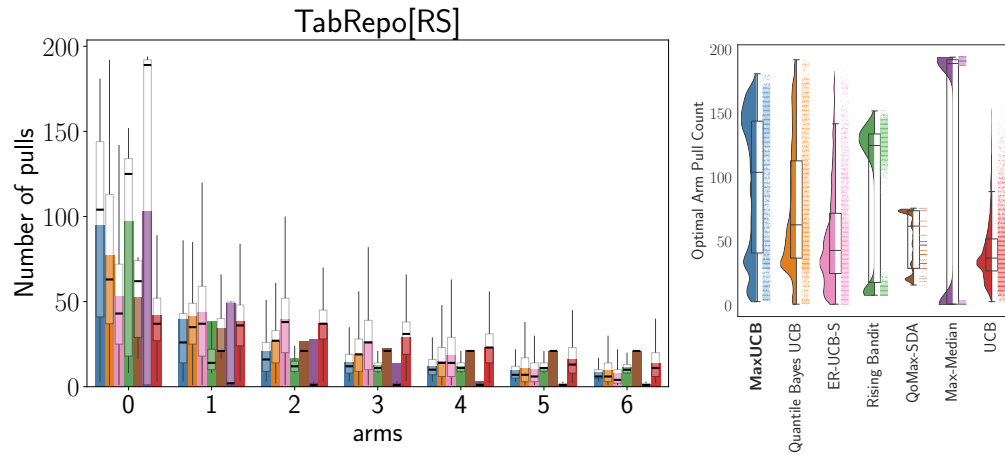


Figure E.1: (Right) The number of all arm pulls, with each bar graph showing the average and the error bars indicating additional statistical information. (Left) The number of best arm pulls for different bandit algorithms.

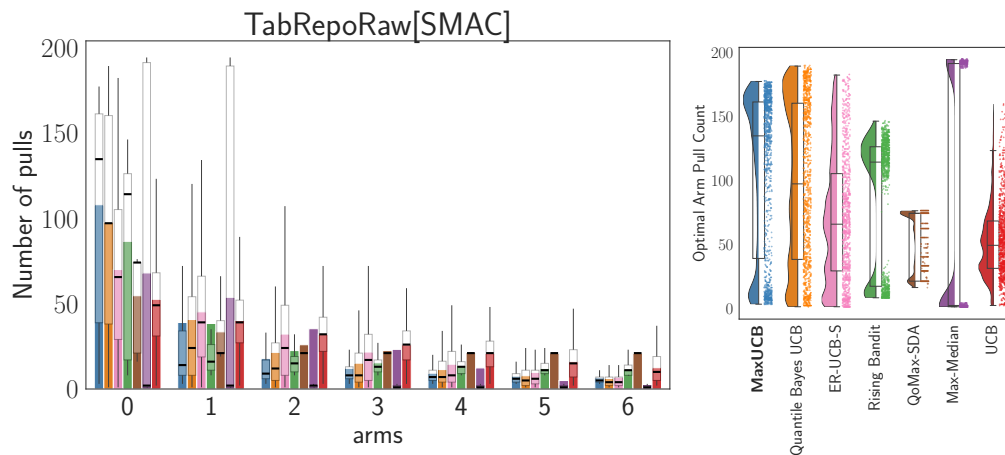


Figure E.2: (Right) The number of all arm pulls, with each bar graph showing the average and the error bars indicating additional statistical information. (Left) The number of best arm pulls for different bandit algorithms.

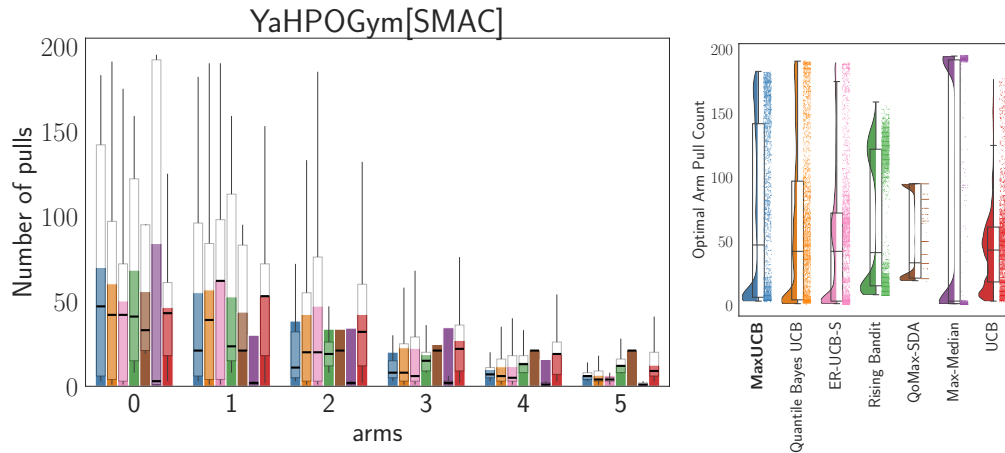


Figure E.3: (Right) The number of all arm pulls, with each bar graph showing the average and the error bars indicating additional statistical information. (Left) The number of best arm pulls for different bandit algorithms.

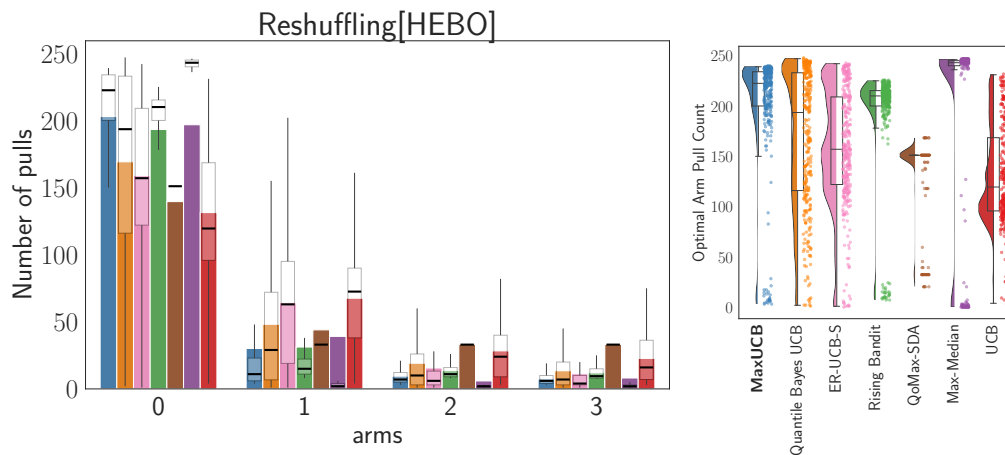


Figure E.4: (Right) The number of all arm pulls, with each bar graph showing the average and the error bars indicating additional statistical information. (Left) The number of best arm pulls for different bandit algorithms.

## E.2 From theory to practice

To validate our theorem against practical outcomes, we applied our algorithm to all benchmarks and plotted the number of pulls for each arm, denoted as "Real Experiment." Additionally, we computed the upper bound on the number of pulls by using the empirical values of  $L_1$  and  $U_i$  and  $\Delta_i$ . Notably, we report the first term of Equation 23 since the second term is nearly constant across all arms according to calculation. The results demonstrate that although the empirical pull counts are much less than the theoretical bounds of Equation 23, both follow a similar decreasing pattern as the rank of suboptimality increases.

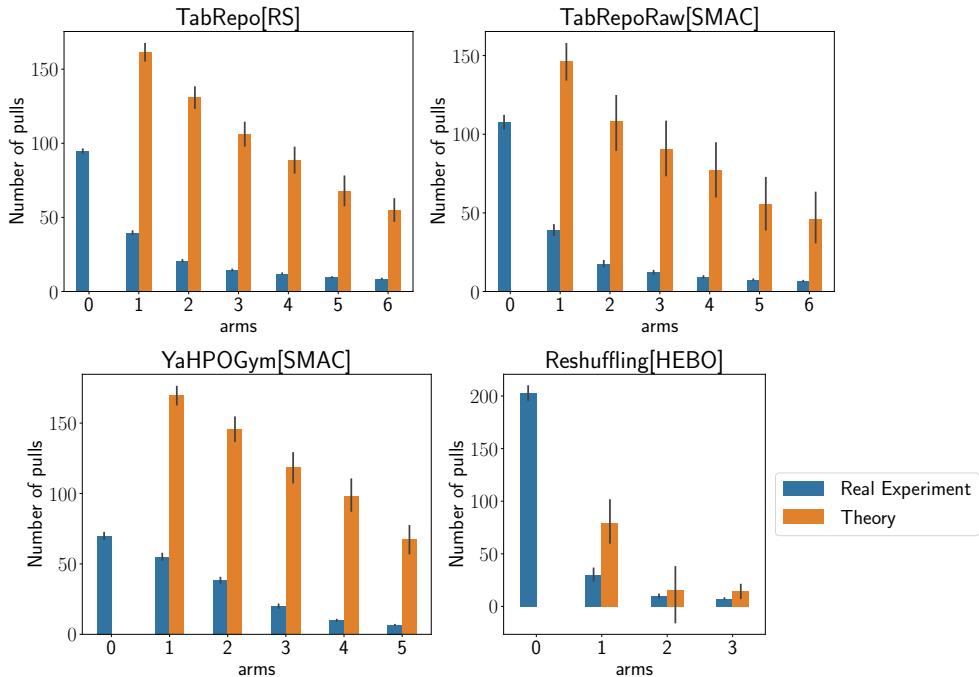


Figure E.5: The number of pulls for each arm in our algorithm, labeled as "Real Experiment" and the theoretical values of this number

## E.3 Addressing Non-stationary Rewards

To handle non-stationary rewards, we pull each arm  $C$  times without observing the rewards before running MaxUCB. This "burn-in" allows the Markov Chain to reach equilibrium, especially from a poor starting point. Algorithm E.1 shows the adapted version of our algorithm. Therefore, empirically, this allows MaxUCB to operate after a fixed exploration phase of all arms until the reward distribution is stationary.

We run Algorithm E.1 with different parameters of  $C \in \{5, 6, 7, 8\}$  using up to 48 iterations corresponding to almost 25% of the total budget. Figure E.6 shows normalized loss per task where columns are sorted by the maximum change of the mean of the reward distributions of the optimal arm computed every 10 HPO iterations (as an indicator of non-stationarity; shown at the top panel in Figure E.6). Figure E.7 shows the average ranking and normalized loss over time for different values of the hyperparameter  $C$ .

The initial burn-in improves final performance for the few tasks where we observe a high shift (right part of Figure E.6) while the initial performance is worse across all tasks (as shown in Figure E.7). However, the results are not sensitive to the exact value of  $C$ . Overall, this naive solution can improve performance for some tasks at the cost of not using potentially valuable information obtained from initial exploration. Thus, optimally addressing non-stationary rewards could be a promising direction for future work.

### Algorithm E.1 MaxUCB-Burn-in

---

**Require:**  $\alpha$ (exploration parameter),  $C$  (burn-in rounds),  $T$ (time horizon),  $K$ (arms) ▷ Burn-in phase

- 1: **for**  $j \leq C$ , **for** each arm  $i \leq K$  **do**
- 2:     Pull arm  $i$
- 3: **end for** ▷ Initial phase
- 4: **for** each arm  $i \leq K$  **do**
- 5:     Pull arm  $i$
- 6:     set  $n_i \leftarrow 1$ , observe reward  $r_{i,1}$
- 7: **end for** ▷ Main phase
- 8: **for**  $t = (CK + K + 1)$  to  $T$  **do**
- 9:     **for** each arm  $i \leq K$  **do**
- 10:         Update policy  $U_i = \max(r_{i,1}, \dots, r_{i,n_i}) + (\frac{\alpha \log(t)}{n_i})^2$
- 11:     **end for**
- 12:     Select arm  $I_t = \arg \max_{i \leq K} U_i$
- 13:      $n_{I_t} \leftarrow n_{I_t} + 1$
- 14:     Observe reward  $r_{I_t, n_{I_t}}$
- 15: **end for**

---

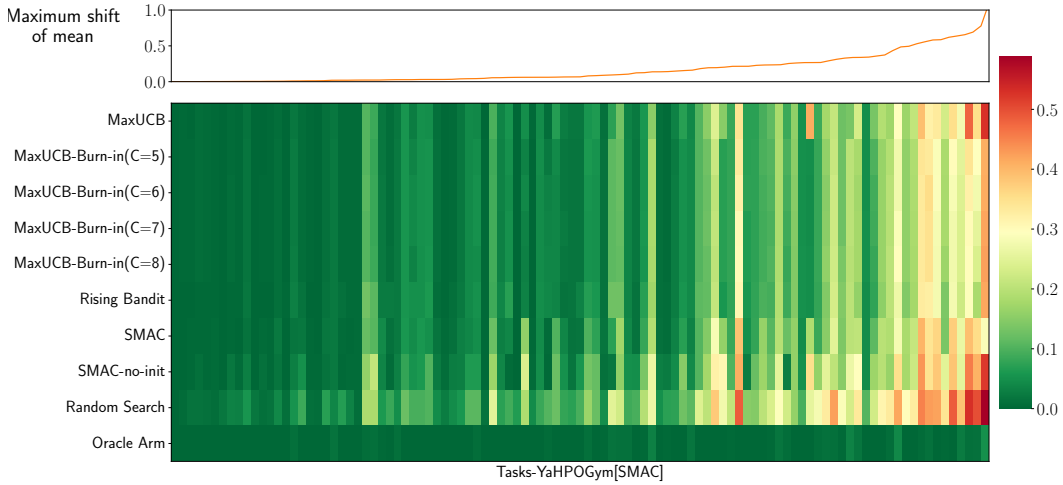


Figure E.6: Heat map shows normalized loss per task, sorted by the distribution shift.

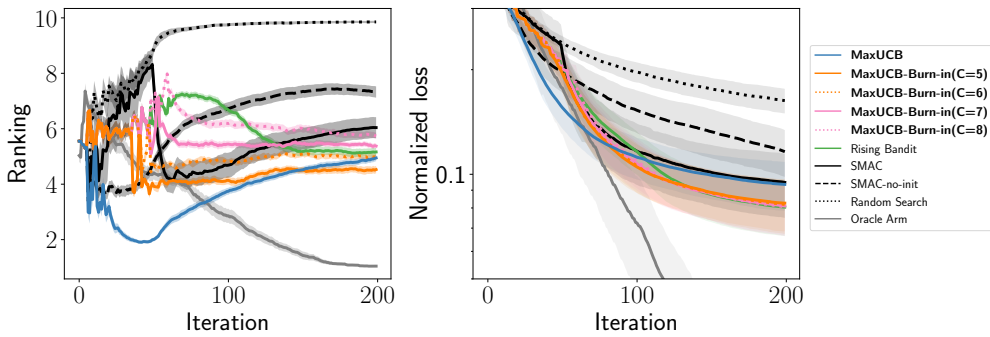


Figure E.7: Average rank and normalized loss of algorithms on YaHPOGym benchmark, lower is better.

## E.4 Toy examples from the extreme bandit’s literature

In this section, we provide additional results on commonly used benchmark functions used in the extreme bandit literature. Concretely, we use a similar setup to [Baudry et al., 2022] and report the following four tasks:

1.  $K = 5$  Pareto distributions with tail parameters parameters  $\lambda_k = [2.1, 2.3, 1.3, 1.1, 1.9]$ . Results are shown in Figure E.8.
2.  $K = 10$  Exponential arms with a survival function  $G_k(x) = e^{-\lambda_k x}$  with parameters  $\lambda_k = [2.1, 2.4, 1.9, 1.3, 1.1, 2.9, 1.5, 2.2, 2.6, 1.4]$ . Results are shown in Figure E.9.
3.  $K = 20$  Gaussian arms, with same mean  $\mu_k = 1, \forall k$ , and different variances  $\sigma_k = [1.64, 2.29, 1.79, 2.67, 1.70, 1.36, 1.90, 2.19, 0.80, 0.12, 1.65, 1.19, 1.88, 0.89, 3.35, 1.5, 2.22, 3.03, 1.08, 0.48]$ . The dominant arm has a standard deviation of 3.35. Results are shown in Figure E.10.
4. (our toy example)  $K = 5$  power distributions with domain parameter  $[3, 4, 5, 5, 4]$  and shape parameter  $[1.01, 1.01, 1.01, 1.1, 1]$ . Results are shown in Figure E.11.

For each task, we run  $N = 1000$  independent repetitions for six time horizons  $T \in \{50100, 200, 500, 1000, 2000\}$ . We show the CDF of the rewards for each arm, the number of times the optimal arm was pulled, and the proxy empirical regret. Notably, the proxy empirical regret is introduced by Baudry et al. [2022] to overcome the issue of high variance in the maximum values of distributions.

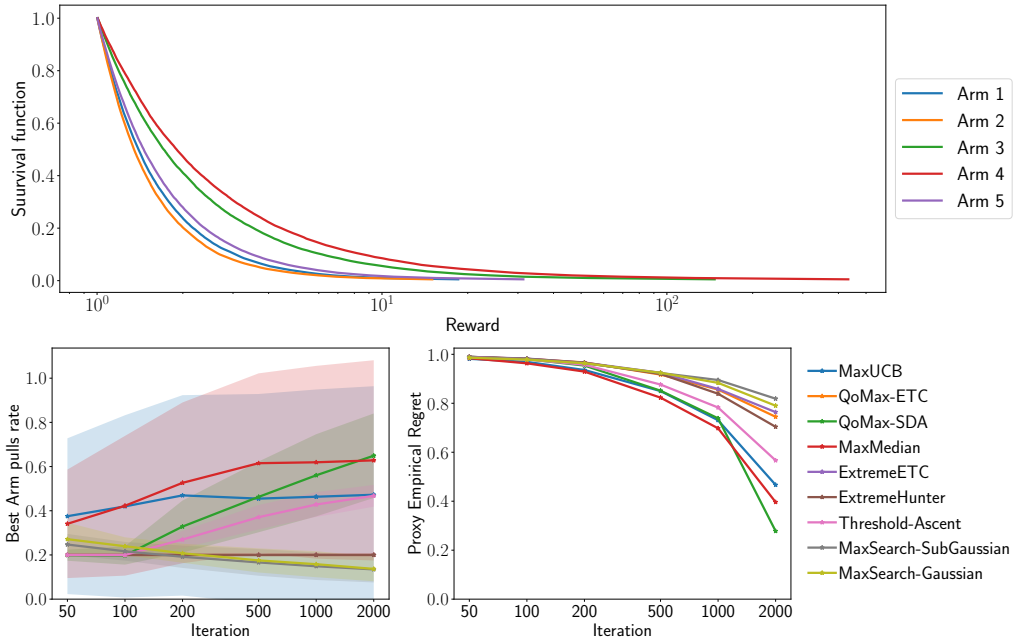


Figure E.8: Experiment 1: (Top) Survival function of distribution of each arm (left) Number of pulls of the optimal arm. (Right) Proxy Empirical Regret

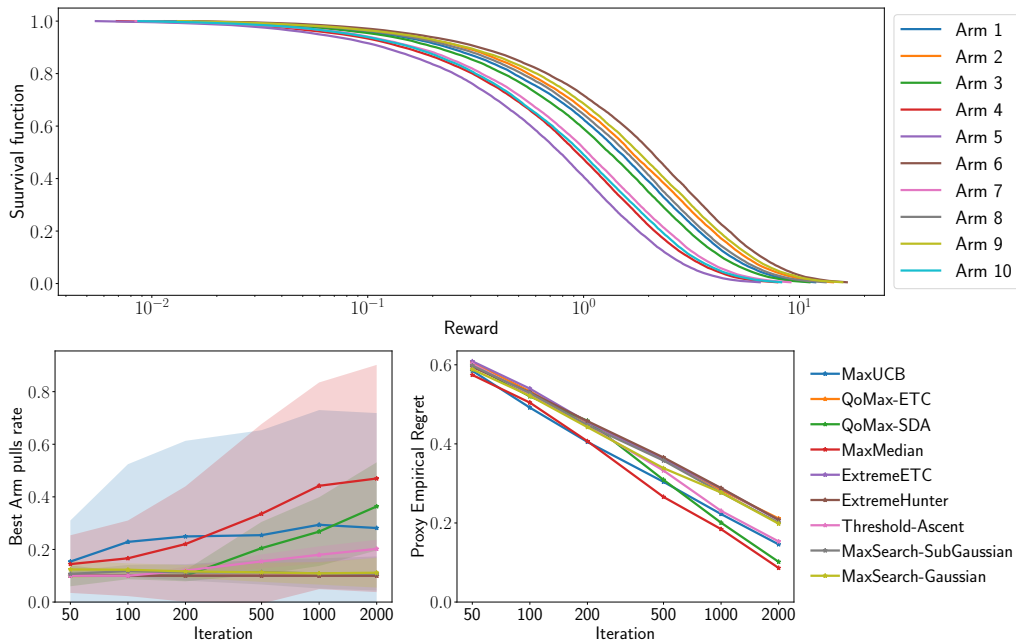


Figure E.9: Experiment 2: (Top) Survival function of distribution of each arm (left) Number of pulls of the optimal arm. (Right) Proxy Empirical Regret

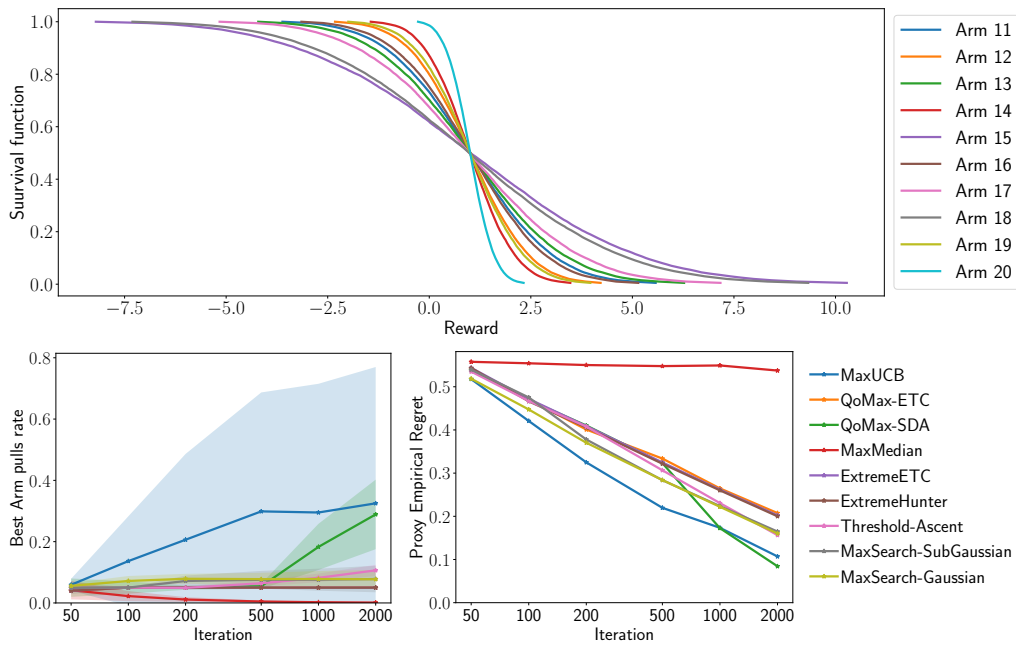


Figure E.10: Experiment 3: (Top) Survival function of distribution of some arms (left) Number of pulls of the optimal arm. (Right) Proxy Empirical Regret

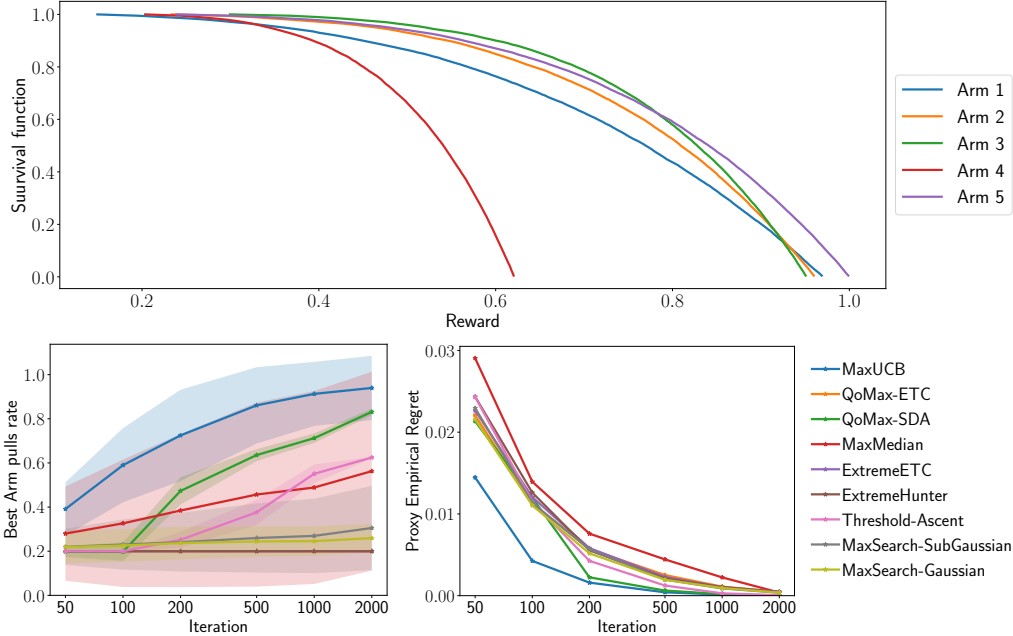


Figure E.11: Experiment 4: (Top) Survival function of distribution of each arm (left) Number of pulls of the optimal arm. (Right) Proxy Empirical Regret

## E.5 Supernet selection in Few-Shot Neural Architecture Search

In one-shot NAS, a single supernet approximates all architectures. However, this estimation could be inaccurate. To address this, few-shot NAS splits the supernet into smaller sub-supernets [Hu et al., 2022, Ly-Manson et al., 2024]. To further improve performance, [Hu et al., 2022] introduced supernet selection, which identifies the most promising sub-supernet and its optimal architecture using techniques such as *Successive Halving*. We aim to identify the best-performing architecture among several subspaces, each corresponding to a sub-supernet. This problem is analogous to the MKB problems, where each arm represents a sub-supernet.

**Dataset Preparation.** We use data provided in [Ly-Manson et al., 2024] for three benchmark datasets: *CIFAR-10*, *CIFAR-100*, and *ImageNet16-120*. Each dataset’s search space is split using 10 different metrics. The splitting follows a binary tree structure with a depth of 3, where operations are divided into two groups at each branch. This process results in 8 sub-supernets per metric. Consequently, for each dataset, we have one full search space and 8 sub-search spaces.

Each combination of dataset and splitting metric is treated as a separate task, yielding a total of 30 tasks (3 datasets  $\times$  10 metrics), each with 8 arms. Following the setup of [Ly-Manson et al., 2024], we randomly sample 600 architectures from both the full search space and each sub-search space. This process is repeated 32 times using different random seeds to ensure variability and robustness in the results.

**Analyzing the reward distribution.** Figure E.12 illustrates the empirical survival functions of the rewards and sub-optimality gaps for the benchmark. As shown, the distribution shape is similar to that of HPO tasks: both are bounded and left-skewed. However, the sub-optimality gap is considerably smaller than HPO tasks, suggesting that identifying the optimal arm is more challenging and may require additional iterations. In Figure E.13, we show values of  $L$  and  $U$  from Lemma 3.3 for this benchmark.

**Performance Analysis.** Figure E.14 presents the average ranking and normalized loss of various bandit algorithms in this benchmark. As shown, *Successive Halving*, *Max-Median*, and *ER-UCB-S* perform well with a small time budget but fail to explore sufficiently to identify the optimal arm. *Rising Bandits*, as a fixed-confidence best-arm identification method, struggles to find the optimal arm. In contrast, MaxUCB outperforms all other baselines, demonstrating better performance when searching the entire search space with a higher budget.

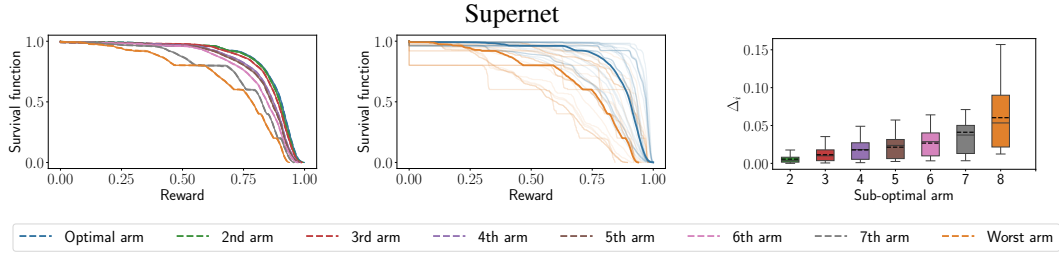


Figure E.12: (Left) The average empirical survival function of the reward (observed performances) per arm ranked per dataset. We divided the reward sequence into five segments over the budget to show the distribution change over time. Thin lines correspond to the survival function of different segments, visualizing the change over time. (Middle) The average ECDF per dataset for the best and worst arm with thin lines corresponding to individual datasets. (Right) The sub-optimality gap  $\Delta_i$ .

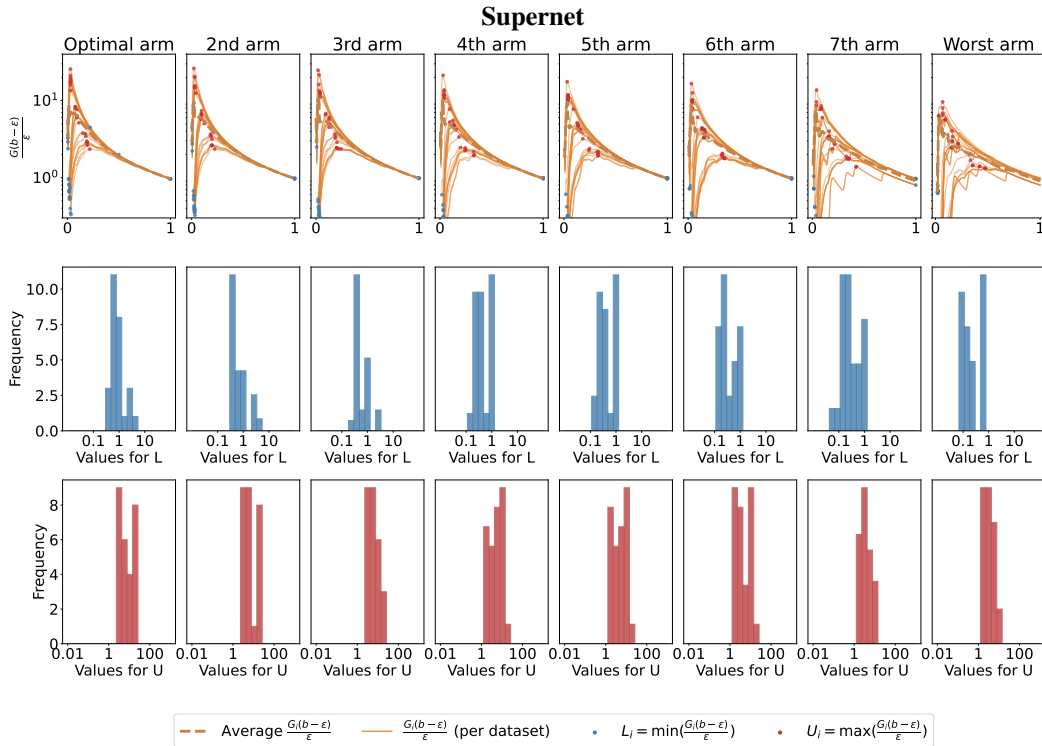


Figure E.13: Arms are ordered by sub-optimality gap. (Top) Thin orange lines represent  $\frac{G(b-\epsilon)}{\epsilon}$ , while the blue and red points correspond to  $L$  and  $U$  for our empirical reward distributions (see Lemma 3.3 for details). (Middle) Histogram of values for  $L$ . (Bottom) Histogram of values for  $U$ .

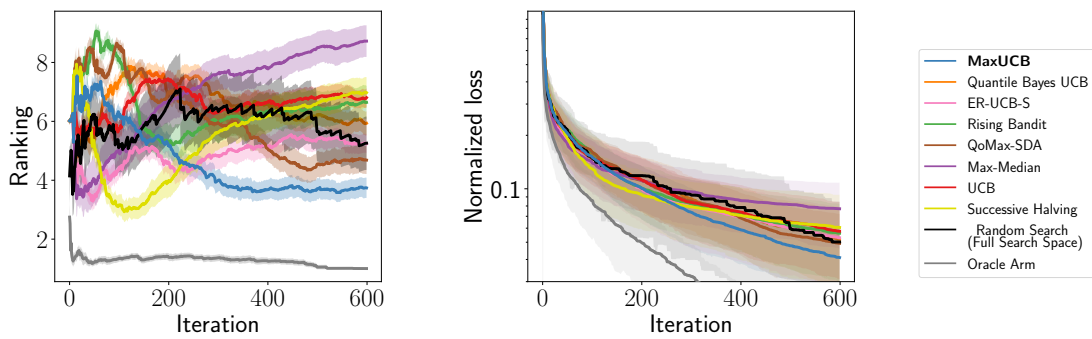


Figure E.14: Average rank and normalized loss of algorithms on *Supernet Selection* benchmark, lower is better.